

This document contains our responses to all reviewer comments, with corresponding references to the text. Additionally, we have attached the second reviewer's comments along with our point-by-point responses, as well as the revised manuscript with all changes highlighted in red.

**RC1:** '[Comment on egusphere-2024-3773](#)', Anonymous Referee #1, 29 Dec 2024 [reply](#)

Luciano Zuccarello et al. provide a comprehensive analysis of the eruptive activity at Stromboli volcano from 3 to mid July 2024. The study utilizes a multi-parameter approach, incorporating seismic, infrasound, and ground deformation data, along with visual and UAS observations, to understand the dynamics of the eruption and its precursors. The study effectively integrates various geophysical data types, providing a holistic view of the eruptive processes.

This multi-parameter approach is crucial for understanding complex volcanic phenomena.

In the manuscript are offered:

1. A detailed chronology of events, from the initial signs of unrest to the paroxysmal eruption on 11 July. This timeline is well-supported by both observational data and geophysical measurements.
2. A clear presentation of the results, with well-constructed figures and tables that enhance the understanding of the data. The use of UAS imagery to complement geophysical data is particularly innovative and provides high-resolution insights into morphological changes.
3. Valuable insights into the eruptive dynamics of Stromboli and similar open-conduit volcanoes. It supports existing models of volcanic activity and highlights the importance of integrated monitoring for eruption forecasting and risk mitigation.

The authors should take into account -mainly for future work- a possible expansion of the discussion to include the broader implications of the findings. How can these insights be applied to other volcanic systems either in Italy or elsewhere? What are the potential impacts on volcanic hazard assessment and mitigation strategies in Arc Volcanoes in the Mediterranean region of similar environments globally?

Overall, the manuscript is a significant contribution to the field of volcanology, providing detailed and valuable insights into the eruptive activity at Stromboli volcano. The soundness of the methodology and the conclusions can be supported by the results, and therefore, I recommend this research paper to be published in its present form.

#### [REPLY](#)

Many thanks for these comments. We have slightly modified the discussion and conclusions to emphasize the vital importance of multiparametric monitoring on conduit volcanoes like Stromboli.

**Citation:** <https://doi.org/10.5194/egusphere-2024-3773-RC1>

**RC2:** '[Comment on egusphere-2024-3773](#)'

The manuscript by Zuccarello et al. addresses a relevant and timely topic both scientifically and in terms of risk management, namely the comprehensive analysis of geophysical signals associated with the eruptive activity of V. Stromboli in July 2024. Added to this is the fact that such activity has been one of the most intense for this volcano in recent years, reaching unprecedented seismic energies and causing severe remodelling of the crater area and northern flank. The chronology and relationship of events and observations made by the authors is very complete and exhaustive. This work is innovative and original, integrating multiparametric data, both public and of their own acquisition, into a well-formulated, simple, clear, coherent methodology based on postulates and physical models appropriate for the object of study. The techniques used are not new or original, but the way of integrating the results and their interpretation for a recent and extraordinary eruptive event is valid and innovative, which is why it is of great interest to the scientific community.

This work completes and advances previous work by some of its authors, providing useful evidence for the conceptual and analytical modeling of the eruptive dynamics of V. Stromboli. The authors carry out a detailed recapitulation, analysis and interpretation of the events and data associated with the eruptive event, based on the state of the art in this matter. It is to be expected that the authors themselves or their collaborators will feed back the existing models on the dynamics of V. Stromboli with these conclusions and that they will effectively be incorporated into the elaboration of their eruptive forecasts.

Below, I detail some particular comments on the different sections and attach the pdf text with some added notes on highlighted lines that I hope can help to further improve this work.

As far as I can assess, the authors make good use of the language. The technical terminology is adequate and precise. A few typos and superscript errors should be corrected for the final version, as well as considering the unification of styles in the date formats used. The illustrations are clear, well defined, and with texts and colours that allow for the good interpretation. I have only left one comment about a figure that is mentioned in the text and has not been incorporated into the preprint. This detail has caused the references to some figures to be wrongly numbered (see comments in the text).

As for the structure of the manuscript, I consider it to be well-designed, ordering the information and its analysis in a coherent manner. The titles of the sections have been appropriately selected and their contents are generally well developed.

The abstract is concise and complete, allowing the objectives and results of the work to be understood in its entirety.

The introduction makes a very exhaustive compilation of the background that justifies and motivates this work and also introduces the reader to the knowledge base of V. Stromboli in an enjoyable way.

Section 2, whose title announces the eruptive chronology from July 3 to 11, begins by describing the activity from May 24. Perhaps the authors could change the title of this section.

Section 3, which refers to the geophysical observations, is too brief and could be expanded with some more detailed information about the instruments used, their characteristics, and the selection of the data for the analysis.

In section 3.1 I have left some comments and suggestions whose consideration would help the reader to better understand the authors' criteria in the analysis of the continuous tremor and the VLPs.

In section 3.2, in addition to verifying the values mentioned in the text and graphs for the frequency ranges used, I have found some differences between the Pa amplitudes in figures 2Sa, 2Sc, and the text.

Section 3.3 lacks the figure mentioned in the text.

The discussion is very rich and well-elaborated based on the results of the analyses of this work and its comparison with previous processes. The conclusions adequately bring together all the information provided, reaching a good synthesis of the results and their scope.

The selected bibliography brings together state-of-the-art on the subject and is generally well-referenced. I have left only a few comments in the text on this subject.

I consider that with some slight modifications to the text and the incorporation of the missing figure, this work is ready to be published and I strongly recommend its inclusion in NHSS

## REPLY

Many thanks for these comments. We have updated the manuscript accordingly. We have addressed the major comments here, while in the attached PDF, we have responded to each individual comment directly within the text.

*Section 2, whose title announces the eruptive chronology from July 3 to 11, begins by describing the activity from May 24. Perhaps the authors could change the title of this section.*

Yes, we agree with you. We have modified the section title to make it more general: 'Chronology of Eruptive Activity'.

*Section 3, which refers to the geophysical observations, is too brief and could be expanded with some more detailed information about the instruments used, their characteristics, and the selection of the data for the analysis.*

We have described the INGV seismo-acoustic network used in this study at the beginning of Section 3.

*In section 3.1 I have left some comments and suggestions whose consideration would help the reader to better understand the authors' criteria in the analysis of the continuous tremor and the VLPs.*

We have added and rephrased some sentences to describe the nature of tremor and VLP (see specific replies in the attached PDF).

*In section 3.2, in addition to verifying the values mentioned in the text and graphs for the frequency ranges used, I have found some differences between the Pa amplitudes in figures 2Sa, 2Sc, and the text.*

Thank you. We have reviewed all the values mentioned in the text. The difference between Figures 2Sa and 2Sc is that the first shows the RMSA, which represents the mean amplitude

over a time window (in this case, 5 minutes), while the second shows the filtered data. The RMSA highlights sustained (long-lasting) events while attenuating individual transient explosions.

*Section 3.3 lacks the figure mentioned in the text.*

Yes, we are not sure why the figure was missing. We have now added it back, showing the tilt reconstructed with the seismometer.

**Citation:** <https://doi.org/10.5194/egusphere-2024-3773-RC2>

- **RC3:** '[Comment on egusphere-2024-3773](#)', Anonymous Referee #3, 22 Jan 2025 [reply](#)

### **Review on Geophysical fingerprint of the 4-11 July 2024 eruptive activity at Stromboli volcano, Italy**

This manuscript presents an extensive study on multi-parameter geophysical data such as seismic, acoustics, and ground deformation during the eruption of Stromboli volcano on 4-11 July 2024. The manuscript gives a good contribution in the field of volcano monitoring and also falls in the scope of NHESS. I think there are several points need to be improved before this manuscript could be accepted for publication.

1. The authors gave a detail and complete information in the introduction of the paroxysmal eruptions of Stromboli volcano, Italy, as well as the preceding eruptive activities and emphasizing the need of multi-parameter geophysical data in the eruption real-time monitoring. However, I found some parts in the introduction to be too extensive. It might be better to move the part of the conceptual models and other geological studies (line 65-76) into the discussion section instead, since the mentioned studies already focus on discussing the possible mechanisms generating paroxysmal eruptions in Stromboli.
2. In Figure 1b, there is no explanation on what N and CS refer to. While later on the text it is mentioned that N refers to the north crater area, it should also be mentioned in the caption of the figure.
3. Wrong station naming in line 128, ISTR3 instead of IST3 as the correct name I presume.
4. The authors used terminology seismic tremor and RMS as interchangeable terms e.g. in the caption of Figure 3a, these two terms have different meaning and could lead into confusion. It is also not clear in the text how the authors defined tremor in their observation. Did they use a threshold in the RMS seismic amplitude to separate tremor from the background energy? Was tremor present continuously all the time on 1-18 July or it started and stopped several time?
5. Figure 4c is too crowded to show the examples of the recorded LP events. I suggest to plot in a shorter time window to show a clear example of one or few recorded LP waveforms.
6. Figure of tilt derived from the seismic data is missing.

7. The authors did not write how they derived tilt from seismic data and only wrote the citations from the former publications which used the same method. For the completeness of the paper, this step needs to be included.

8. Figure 7 is missing.

9. The format used for date throughout the text is not uniform, for instance 4 July, 2024 on line 18 and July 7 on line 19. Please use the uniform date format throughout the manuscript.

10. I would prefer to separate the discussion into several sub-sections, for example separating the discussion of early eruption until the major explosion on 4 July, and then the paroxysmal eruption on 11 July. The interpretation of the observation and possible model from the literature studies could be discussed in each respective sub-section. This way, the discussion could become more focus and easier to follow.

## REPLY

Many thanks for these comments. Below, you will find replies to each comment.

*1. The authors gave a detail and complete information in the introduction of the paroxysmal eruptions of Stromboli volcano, Italy, as well as the preceding eruptive activities and emphasizing the need of multi-parameter geophysical data in the eruption real-time monitoring. However, I found some parts in the introduction to be too extensive. It might be better to move the part of the conceptual models and other geological studies (line 65-76) into the discussion section instead, since the mentioned studies already focus on discussing the possible mechanisms generating paroxysmal eruptions in Stromboli.*

We agree with your comment. We have smoothed and refined the introduction, particularly the paragraph on the models. Some aspects of the model are further discussed in the main text, as noted in our response to comment 10. Thank you.

*2. In Figure 1b, there is no explanation on what N and CS refer to. While later on the text it is mentioned that N refers to the north crater area, it should also be mentioned in the caption of the figure.*

We have modified the caption. Thank you.

*3. Wrong station naming in line 128, ISTR3 instead of IST3 as the correct name I presume.*

Done, thank you.

*4. The authors used terminology seismic tremor and RMS as interchangeable terms e.g. in the caption of Figure 3a, these two terms have different meaning and could lead into confusion. It is also not clear in the text how the authors defined tremor in their observation. Did they use a threshold in the RMS seismic amplitude to separate tremor from the background energy? Was tremor present continuously all the time on 1-18 July or it started and stopped several time?*

Yes, the terminology was probably misleading. We have updated the text to use 'RMS tremor amplitude.' There is no threshold to separate the tremor from the background energy; we simply calculated the RMS within the tremor frequency range (1-3 Hz). Therefore, the tremor was recorded throughout the period, but with varying amplitudes, as explained in the text.

5. *Figure 4c is too crowded to show the examples of the recorded LP events. I suggest to plot in a shorter time window to show a clear example of one or few recorded LP waveforms.*

We have modified the figure showing just 20 minutes of July 3, where multiple LP events occurred. Thank you.

6. *Figure of tilt derived from the seismic data is missing.*

Yes, it's missing. We have added it.

7. *The authors did not write how they derived tilt from seismic data and only wrote the citations from the former publications which used the same method. For the completeness of the paper, this step needs to be included.*

We agree. We have rephrased the sentence adding more information that explains briefly how it's working: 'The relationship between displacement and tilt sensitivities is a function of the long-period corner frequency of the seismometer used. By applying the magnification factor (e.g., Aoyama et al. (2008), Genco and Ripepe (2010), and De Angelis and Bodin (2012)), which is constant around the natural period of the seismometer, we were able to convert the seismometer's output from displacement to ground tilt'.

8. *Figure 7 is missing.*

We have added it.

9. *The format used for date throughout the text is not uniform, for instance 4 July, 2024 on line 18 and July 7 on line 19. Please use the uniform date format throughout the manuscript.*

Thank you for this comment. We have standardized the text by adopting the journal's guidelines, using the format 'day month, year' and 'day month'.

10. *I would prefer to separate the discussion into several sub-sections, for example separating the discussion of early eruption until the major explosion on 4 July, and then the paroxysmal eruption on 11 July. The interpretation of the observation and possible model from the literature studies could be discussed in each respective sub-section. This way, the discussion could become more focus and easier to follow.*

We agree with this comment. We have divided the discussion into three subsections following a brief introduction: the first week of July, the second week of July, and the morphological changes in the crater area caused by the explosive activity. Each subsection discusses the eruptive models from the literature. Thank you.

**Citation:** <https://doi.org/10.5194/egusphere-2024-3773-RC3>



# Geophysical fingerprint of the 4-11 July 2024 eruptive activity at Stromboli volcano, Italy.

Luciano Zuccarello<sup>1,2</sup>, Duccio Gheri<sup>1</sup>, Silvio De Angelis<sup>2,1</sup>, Riccardo Civico<sup>3</sup>, Tullio Ricci<sup>3</sup>, Piergiorgio Scarlato<sup>3</sup>.

<sup>1</sup>Istituto Nazionale di Geofisica e Vulcanologia, Sezione di Pisa, via Cesare Battisti, 53, 56125, Pisa, Italy.

<sup>2</sup>School of Environmental Sciences, University of Liverpool, 4 Brownlow Street, L69 3GP, Liverpool, UK.

<sup>3</sup>Istituto Nazionale di Geofisica e Vulcanologia, Sezione di Roma1, via di Vigna Murata, 605, 00143, Roma, Italy.

*Correspondence to:* Luciano Zuccarello (luciano.zuccarello@ingv.it); Duccio Gheri (duccio.gheri@ingv.it)

**Abstract.** Paroxysmal eruptions, characterized by sudden and vigorous explosive activity, are common events at many open-vent volcanoes. Stromboli volcano, Italy, is well-known for its nearly continuous degassing activity and mild explosions from the summit craters, occasionally punctuated by energetic, short-lived paroxysms. Here, we analyse multi-parameter geophysical data recorded at Stromboli in early July 2024, during activity that led to a paroxysmal eruption on 11 July. We use seismic, infrasound and ground deformation data, complemented by visual and Unoccupied Aircraft System observations, to identify key geophysical precursors to the explosive activity and reconstruct the sequence of events. Elevated levels of volcanic tremor and Very Long Period (VLP) seismicity accompanied moderate explosive activity, lava emission and small collapses from the north crater, leading to a major explosion on 4 July 2024 at 12:16 (UTC). Collapse activity from the North crater area continued throughout July 7, while effusive activity occurred from two closely-spaced vents located on the Sciara del Fuoco slope, on the Northwest flank of the volcano. On 11 July, a rapid increase in ground deformation preceded, by approximately 10 minutes, a paroxysmal event at 12:08 (UTC); the explosion produced a 5 km-high eruptive column and pyroclastic density currents along Sciara del Fuoco. We infer that the early activity in July was linked to eruption of resident magma within the shallowest parts of the volcano plumbing. This was followed by lowering of the magma level within the conduit system as indicated by the location of newly opened effusive vents. The rapid inflation observed before the paroxysmal explosion on 11 July is consistent with the rapid expansion of gas-rich magma rising from depth, as frequently suggested at Stromboli during energetic explosive events. Our results provide additional valuable insights into the eruptive dynamics of Stromboli and other open-conduit volcanoes, and emphasize the importance of integrated geophysical observations for understanding eruption dynamics, their forecasting and associated risk mitigation.

## 1 Introduction

Stromboli is an open conduit stratovolcano located in the Tyrrhenian Sea, off the northern coast of Sicily; its activity is characterized by continuous degassing and frequent, small-to-moderate, explosions occurring every few minutes from the summit craters, the well-known Strombolian activity. However, activity at Stromboli can rapidly escalate into more energetic





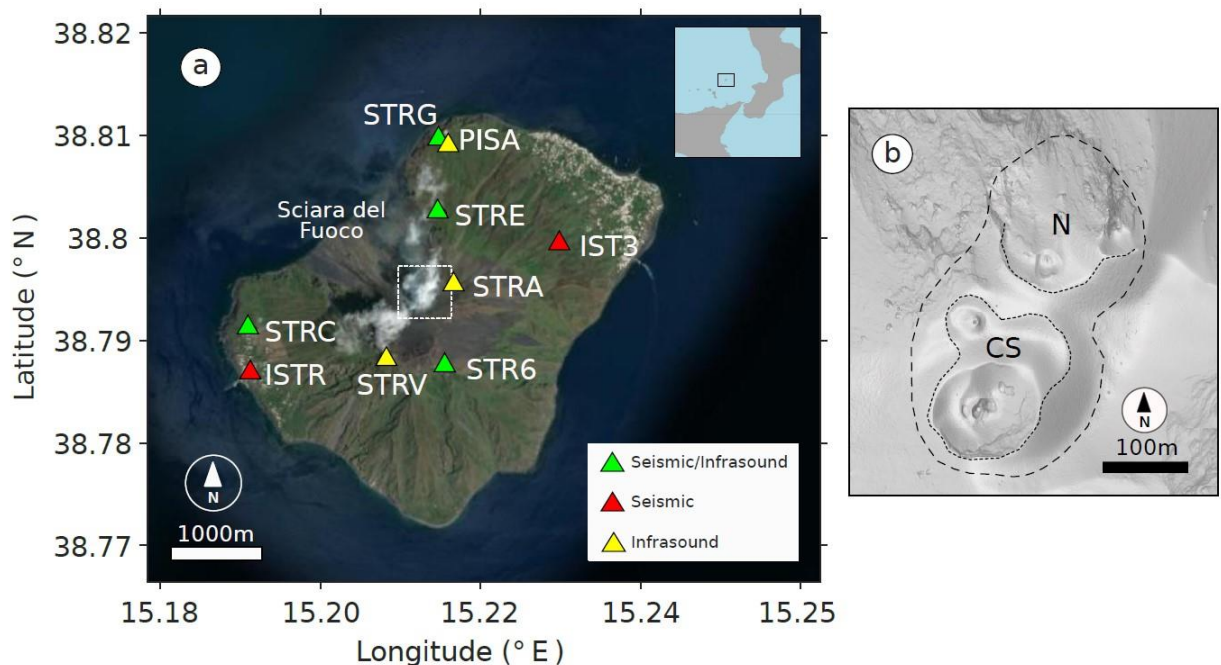
32 events, referred to as major explosions, which eject centimeter-to-meter-sized ballistic projectiles; at times, sustained explosive  
 33 activity is accompanied by partial collapses of the crater rim due to the instability of accumulated material, and increased  
 34 magmatic pressure within the conduit system (Gurioli et al., 2013; Di Traglia et al., 2024). Since 2019, major explosions at  
 35 Stromboli have occurred with a frequency of about 4-5 events per year ejecting pyroclastic material to heights over a hundred  
 36 meters, which can travel beyond the summit crater area and potentially affect tourist paths (Rosi et al., 2013; Gurioli et al.,  
 37 2013). In heightened states of activity, Stromboli may also experience paroxysms, that is highly energetic eruptions that  
 38 generate eruptive columns exceeding 4 km in height, ballistics of up to 2 m in diameter and significant collapse activity from  
 39 the summit crater areas (Fig. 1). Paroxysms can be accompanied by the emplacement of pyroclastic density currents (PDCs)  
 40 along the Sciara del Fuoco (SdF, Fig. 1a), which can enter the sea and travel up to 2 km from the shoreline with demonstrated  
 41 potential to trigger tsunamis (Rosi et al., 2006; Calvari et al., 2006; D'Auria et al., 2006; Ripepe and Lacanna, 2024). Although  
 42 paroxysms are less frequent than major explosions, with an average occurrence of just one every four years since 2003, they  
 43 are the most impactful hazard for the island of Stromboli (Rosi et al., 2013). A recent paroxysm on 3 July, 2019, resulted in a  
 44 fatality (Giudicepietro et al., 2020; Giordano and De Astis, 2020; Andronico et al., 2021).  
 45 Unrest and eruption at Stromboli generate a broad range of geophysical signals. Nucleation and coalescence of gas bubbles  
 46 into gas slugs (Sparks, 2003; Burton et al., 2007; Caricchi et al., 2024), and their ascent within the conduit generates  
 47 characteristic seismic and deformation signals (Marchetti et al., 2009); gas slug bursting at the top of the magma column  
 48 produces infrasound waves (Colò et al., 2010). Real-time detection and monitoring of these signals are crucial for risk  
 49 mitigation at Stromboli as, in the recent past, major explosions and paroxysms have frequently been anticipated by detectable  
 50 changes in geophysical signals between tens of seconds and minutes before their occurrence (Giudicepietro et al., 2020; Ripepe  
 51 et al., 2021a; Longo et al., 2024).  
 52 Except for the 2019 eruptive activity, the most intense in recent years, Stromboli's paroxysms are typically preceded by periods  
 53 of lava effusion, or a general increase in surface activity that lasts for several days (Ripepe et al., 2009; Valade et al., 2016).  
 54 Several studies have suggested that effusive eruptions may act as a trigger for paroxysmal explosions through a mechanism of  
 55 decompression of the volcano plumbing system, evidenced by a drop in magma levels within the conduit (Aiuppa et al., 2010;  
 56 Calvari et al., 2011; Ripepe et al., 2017). The most significant effusive event in terms of its volume occurred between December  
 57 2002 and July 2003 (Ripepe et al., 2017), which caused landslides, triggered a partial collapse of the SdF and culminated in a  
 58 paroxysm on 5 April, 2003; this was the first large-scale paroxysmal event on record since 1985 (Calvari and Nunnari, 2023).  
 59 However, it should also be noted that effusive eruptions are not necessarily followed by paroxysms. An example is the  
 60 November 2014 effusive eruption, which did not lead to paroxysmal activity (Rizzo et al., 2015). At the other end of the  
 61 spectrum lies the paroxysm of July 2019, for which no clear increase in activity prior to the main event was recorded. As  
 62 highlighted by Laiolo et al. (2022), thermal and gas flow levels had slightly increased but remained below "alert" thresholds.  
 63 Multi-parameter data are crucial to understand unrest at Stromboli and to detect transitions between low-to-moderate activity  
 64 and more explosive phases (Pistolesi et al., 2011; Andronico et al., 2021). Several conceptual models have been proposed  
 65 accounting for the ordinary seismic activity observed at Stromboli and other similar volcanoes (e.g., Chouet et al., 2008;





66 Suckale et al., 2016; Ripepe et al., 2021b). Petrological analyses of erupted products suggest the presence of a stratified conduit  
67 at Stromboli, consisting of two types of magma (Bertagnini et al., 2003; Francalanci et al., 2004; Francalanci et al., 2005). The  
68 upper conduit is thought to host highly porphyritic (HP) magma that is water-poor and rich in phenocrysts, and is erupted as  
69 scoria during ordinary activity; on the other hand, magma in the lower conduit is gas-rich, low-porphyritic (LP), and typically  
70 erupted as pumice alongside HP scoria and lithic blocks removed from conduit walls. Eruptive activity at Stromboli is inferred  
71 to be controlled by the buoyant ascent and bursting of gas slugs (Sparks, 2003; Burton et al., 2007; Caricchi et al., 2024;  
72 Aiuppa et al., 2010) from the top of the LP magma, rising through the more crystalline HP magma acting like a viscous fluid  
73 or a rigid plug and controlling the final ascent and explosion of the slugs (Suckale et al., 2016). A recent model by (Caricchi  
74 et al., 2024) shows that the instability of gas-rich and low-density foam layers at the base of the magma column could also  
75 potentially trigger paroxysmal explosions at open conduit volcanoes.

76 In this study, we report on the most recent paroxysm at Stromboli, which occurred on 11 July 2024, after a month of unrest at  
77 the summit craters, as reported by the Istituto Nazionale di Geofisica e Vulcanologia (INGV) (INGV-OE, 2024). We analyze  
78 the precursory geophysical activity leading up to the paroxysm based on seismic, infrasound and ground deformation data  
79 gathered by the INGV monitoring network, complemented by observations conducted with an Unoccupied Aircraft System  
80 (UAS) during the study period. The UAS imagery provides a valuable tool to interpret geophysical data and understand the  
81 conditions leading up to the paroxysm on 11 July, offering a high-resolution reconstruction of the eruptive events and  
82 associated morphological changes at the volcano. Unless, otherwise stated, all descriptions of surface activity in this  
83 manuscript are from direct field observations by the authors during the study period.





85 **Figure 1: a) Map of monitoring network at Stromboli, showing the locations of seismo-acoustic, seismic, and infrasound sensors.**  
 86 **The inset shows the location of Stromboli volcano in Italy (MATLAB-Mapping Toolbox). b) Detail of the summit area of Stromboli,**  
 87 **corresponding to the white dash-line square in a), showing the summit crater areas.**

## 88 2 Chronology of eruptive activity during 3-11, July, 2024

89 The activity bulletins issued by INGV (see Data Availability), from May 24 until the early days of July, reported an increase  
 90 in surface activity at Stromboli, particularly from the North (N) crater area (Fig. 1b), characterized by continuous and intense  
 91 spattering, that is quasi-continuous emission of pyroclastic material through sequential, small-to-moderate, explosions ejecting  
 92 ballistics at heights of ~10-20 m above the vent (Harris and Ripepe, 2007; Giudicedipietro et al., 2021) (Fig. 2a). The average  
 93 frequency of explosions fluctuated between 13 (medium) and 16 (high) events/hour with spattering occasionally leading to  
 94 lava flows along the SdF (Fig. 1a). On June 23 and 28, lava flows began, following intense spattering from the N crater,  
 95 converging into a canyon-like structure created by previous PDC activity in October 2022 (Di Traglia et al., 2024). Sulfur  
 96 dioxide (SO<sub>2</sub>) and carbon dioxide (CO<sub>2</sub>) emissions remained at average levels, as did the carbon-to-sulfur (C/S) ratio (INGV-  
 97 OE, 2024).

98 On 3 July, at 16:35 UTC, intense spattering was observed from a vent located within the N crater sector, leading to a sequence  
 99 of partial collapses of the N crater rim, which also remobilized material that had been erupted in the preceding days. These  
 100 collapses mostly consisted of cold material with a minor contribution of hot deposits. At 17:02 UTC, a lava flow began from  
 101 the same vent, accompanied by spattering and moderate explosions (Fig. 2b). The activity continued throughout the night, with  
 102 lava fronts moving down to an elevation of 550-600 m a.s.l..

103 On 4 July, at 12:16 UTC, a major explosion occurred from the N crater and, at 14:10 UTC, a new lava flow emerged at the  
 104 base of the N crater area at ~700 m a.s.l., advancing towards Bastimento and Filo di Fuoco, located along the northeast  
 105 boundary of SdF. After about one hour a second lava flow started at an elevation of ~580 m a.s.l., which reached the sea. At  
 106 16:15 UTC, another vent opened at ~510 m a.s.l., producing a third lava flow accompanied by PDCs that rapidly descended  
 107 the SdF into the sea (Fig. 2c). During the evening of 4 July, and throughout the following night, lava flow activity continued,  
 108 accompanied by occasional collapses of pyroclastic materials.

109 Between 5-6 July, 83 landslide events were observed, while effusive activity fluctuated and lava emission moved further  
 110 downslope originating from two new eruptive vents at ~485 m a.s.l. (Fig. 2d). The flow formed a delta at the shoreline and  
 111 steam plumes were observed caused by magma-seawater interaction. Explosive activity from the summit craters halted at the  
 112 beginning of the effusive phase.

113 On 11 July, at 12:08 UTC, a paroxysmal eruption occurred from the N crater area, producing an ash plume ~5 km high,  
 114 which dispersed towards the southwest (Fig. 2e). Shortly after, a pyroclastic flow rapidly advanced along the SdF, which  
 115 triggered a small-scale tsunami wave. The paroxysmal phase ended with a series of secondary and less intense PDCs.

116 In the following hours, effusive activity ceased, and no further explosions were observed, except for a minor event on 12 July,  
 117 at 08:28 UTC (Fig. 2a), which was followed by a small collapse event in the N crater area.

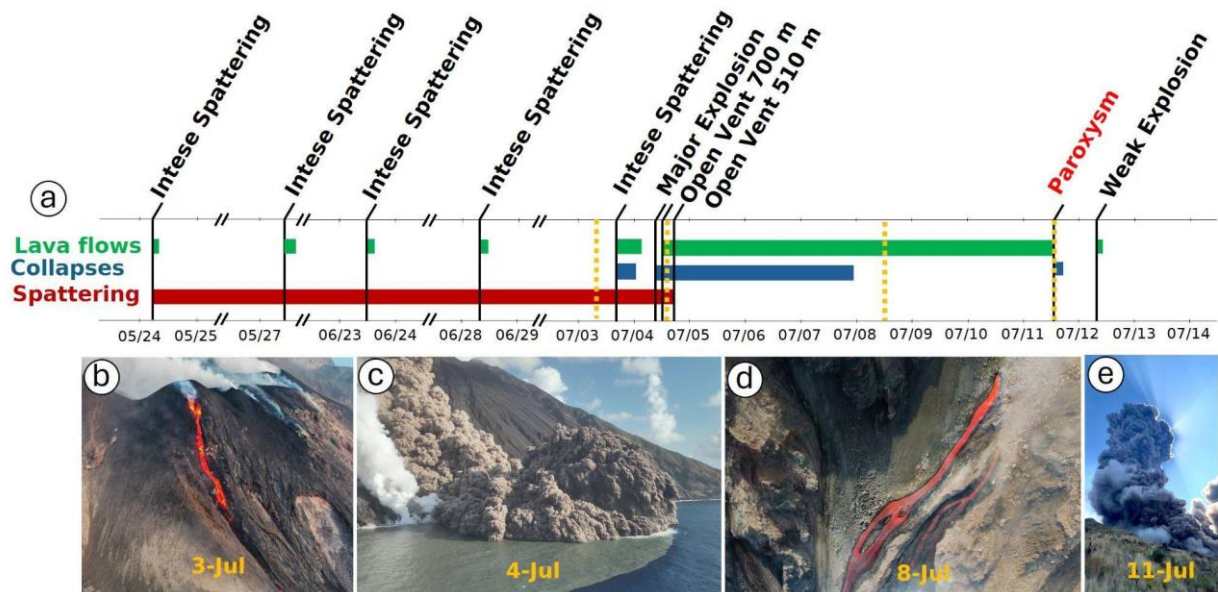


**Figure 2: Timeline of the observed surface activity and key visual observations at Stromboli between late May and mid-July, 2024.**  
a) Timeline showing the chronology of activity, which marks periods of activity characterized by lava flows (green), collapses (blue) and spattering (red). Significant events are labelled, such as intense spattering, a major explosion on 4, July, opening of new vents, and the paroxysm on 11, July. b-e) Sequence of images gathered at the times indicated by the dashed yellow lines in a). From left to right: spattering activity on 3, July, a PDC event reaching into the sea on 4, July, continued lava flow on 8, July, and the paroxysmal explosion on 11, July (photo “e” courtesy of G. De Rosa - OGS).

### 3 Geophysical observations

In this study we use data recorded by the geophysical monitoring network deployed and maintained on Stromboli by INGV (Fig. 2a). The network includes seismic (ISTR3, ISTR) and infrasound sensors (STRA, STRV), as well as seismo-acoustic stations (STR6, STRC, STRE, STRG). An additional infrasound sensor, PISA (Gheri et al., 2024), was deployed on 4 July at 13:35 UTC, 35 minutes before the onset of the effusive activity.

#### 3.1 Seismic characterization of unrest and eruptive events

Volcanic tremor is traditionally thought to reflect magma movement within the conduit (McNutt and Nishimura, 2008; Chouet et al., 1997; Ripepe and Gordeev, 1999); at Stromboli, tremor is routinely monitored by means of the Root Mean Square (RMS) of the continuous seismic signal in the 1-3 Hz frequency band (Giudicepietro et al., 2023). Figure 3a shows RMS values of the order of 10-6 ms-1 (recorded at the ISTR3 site), which correspond to tremor classified by INGV as high. A marked and short-lived increase in seismic RMS was observed after the major explosion at 12:11 on 4 July (Fig. 3a). During this period, the signal reached unprecedented levels, peaking at 1.4 ms-1 at 17:00 UTC. Short-lived increases in RMS values were still noted



137 throughout 5, July, although the amplitudes exhibited an overall decline to values of the order of  $10^{-7} \text{ m s}^{-1}$ , lower than those  
138 recorded at the beginning of July. In the following days (6-11, July), the tremor was marked by a series of short-duration peaks  
139 during lava flow activity. This behavior changed again on 11, July, when the onset of paroxysmal activity coincided with a  
140 new increase in RMS (Fig. 3a). After the paroxysm, the RMS decreased again with only sparse and brief intervals of increased  
141 amplitudes between 12-13, July (Fig. 3a). From late on 13 July, onwards, the amplitude stabilized around  $10^{-7} \text{ m s}^{-1}$ , indicating  
142 that volcanic activity had reduced and returned to background levels. Additional details of the signals recorded on 4-7 July,  
143 are shown in the Supplementary Materials (Fig. 1S).

144 The spectrogram in Fig. 3b shows nearly continuous energy in the 2-3 Hz range, typically associated with tremor signals at  
145 Stromboli (Ripepe et al., 1996). Energy levels in this band change throughout the pre-, syn-, and post-explosive activity  
146 periods, reaching a maximum on 4 July following the major explosion. A pulsating phase was observed from 6-11 July, with  
147 another peak during the paroxysm. Explosive activity between 4-11, July, exhibited a broader frequency range in the 0.5-15  
148 Hz band. It is worth noting that the eruptive event on 4, July was preceded by a high-energy signal in the narrow frequency  
149 band 0.2-0.3 Hz (Fig. 3b). We also observe that this very low-frequency signal was not recorded before the paroxysm on 11,  
150 July. Finally, on July 10 at 05:09 UTC and on 11 July at 02:26 and 15:21 UTC, high-energy signals were observed around  
151 0.05-0.08 Hz, exhibiting a dispersive spectrum typical of teleseismic events as reported by USGS (for further information, see:  
152 <https://earthquake.usgs.gov/earthquakes/search/>).

153 We have also analysed the occurrence of Very Long Period (VLP) earthquakes that have traditionally been associated with  
154 pressure disturbances and the dynamics of gas-rich magma within fluid-filled structures (Chouet et al., 1997; Chouet et al.,  
155 1999; Marchetti and Ripepe, 2005; Legrand and Perton, 2022), and one of the main tools used to monitor unrest at Stromboli.  
156 An increase in the frequency of occurrence of these signals is typically a precursor to periods of elevated eruptive activity  
157 (Ripepe et al 2009; Delle Donne et al., 2017). Figure 4a derived from information sourced from the INGV bulletins (INGV-  
158 OE, 2024), provides an overview of the rates of VLP seismicity at Stromboli between the end of May and mid-July 2024, after  
159 the 11 July paroxysm. From May until mid-June, VLP event rates remained stable, fluctuating around high values between 12  
160 and 19 events/hour. A mean rate of  $\sim 13$  events/hour is defined, at Stromboli, as “normal activity” (Ripepe et al., 2008) and it  
161 suggests that an efficient degassing mechanism of the magma column is established (Ripepe et al., 2021b). A significant peak  
162 is observed around mid-June, with the number of VLP events reaching a high of 19 events/hour on June 16. This peak is  
163 followed by a slight decrease in event rates, although the number of events remained elevated compared to previous days.  
164 Figure 4b shows the characteristic compression-decompression cycle of VLP events at Stromboli; this waveform represents  
165 the normalized stack of all VLP events with maximum amplitude greater than  $5 \times 10^{-6} \text{ m s}^{-1}$  at station STRE. Figure 4c shows  
166 a 1-day filtered (0.03-3Hz) seismic record illustrating the occurrence of VLP events as recorded at station STRE, on the east  
167 flank of SdF at 495 m of elevation (see Fig. 1).

168 Before the major explosion on 4 July, we observed a clear drop in the occurrence of VLP events (Fig. 4a) from 10-15 to 7-10  
169 events/hour. The rates of VLP events remained stable until the 11 July paroxysm, peaking again at 12 events/hour on that day.  
170 After the paroxysm, a further decrease in VLP rates was observed with hourly counts ranging from 6 to 10 events.



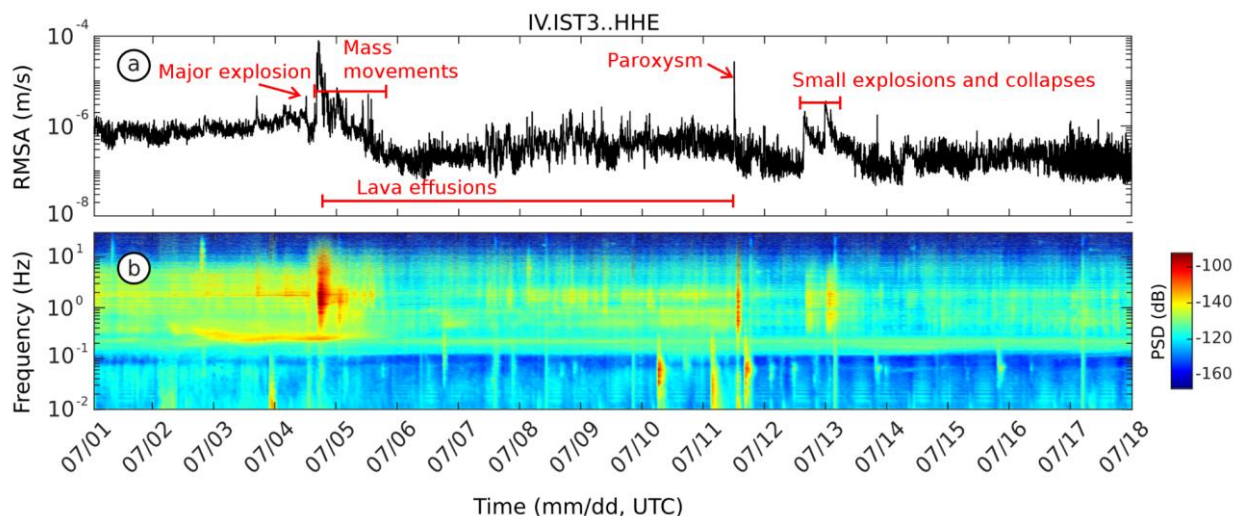


**Figure 3: a) Seismic tremor or RMS calculated every minute using a moving time window of 5 minutes, within the volcanic tremor frequency band of Stromboli (1-3 Hz), from July 2 to 18. b) Spectrogram of the E-component from the IST3 seismic station for the same period.**

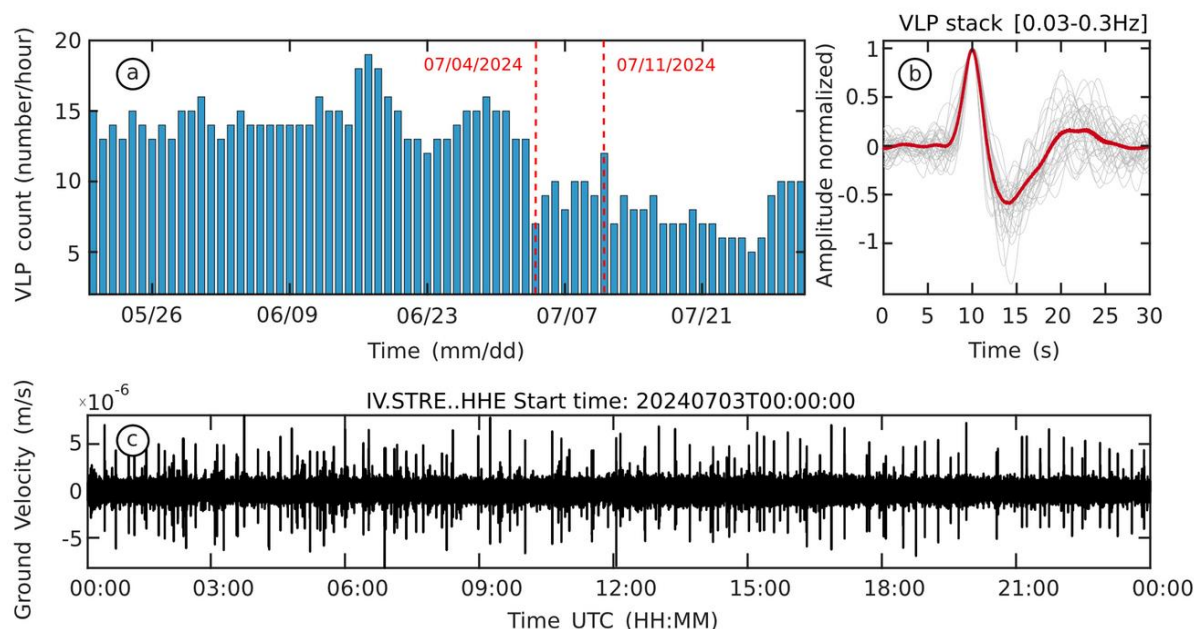


**Figure 4: a) Hourly rates of VLP events from the INGV catalog. Vertical red dashed lines indicate the major explosion and paroxysm that occurred on 4 and 11, July, respectively. b) VLP waveform events ( $>5 \times 10^{-6}$  m s $^{-1}$ ) recorded on 3, July, at station STRE normalized with respect to maximum amplitude (light grey). The red waveform represents the average of all high-amplitude waveforms. c) Continuous waveform recorded at station STRE (EW component) on 3, July 2024, filtered between 0.03-0.3 Hz.**



### 3.2 Infrasound characterization of unrest and eruptive events

We have also analysed infrasound data recorded by the INGV acoustic monitoring network and an additional microphone installed during the period of activity (Fig. 1). The infrasonic record before 4, July, shows a typical background of moderate strombolian activity occasionally interspersed with larger explosions (see Fig. 2Sa). The major explosion on 4 July, generated an infrasonic transient with a pressure of 5 Pa (Fig. 2Sb) at station STR6, from the CS crater area. Following this event, a marked decrease in acoustic energy was observed until the 11, July paroxysmal event, which produced infrasonic waves with a peak amplitude of 115 Pa at the STR6 site (approximately at ~750 m, see Fig. 1a and Fig. 2Sb).

We have used the infrasound records from all operating sensors of the INGV monitoring network on Stromboli and an additional temporary microphone (Fig. 2) to locate the source of the paroxysmal eruption on 11, July 2024. We employed the RTM-FDTD (Reverse Time Migration - Finite Difference Time Domain) method of Fee et al. (2021), which implements waveform back-projection over a grid of candidate source locations. Travel-times between potential source locations and all stations in the network are calculated via FDTD modeling (Kim and Lees, 2014; Fee et al., 2017; Diaz-Moreno et al., 2019) to account for the effect of topography on the propagation of the acoustic wavefield. In the RTM-FDTD method, waveforms are back-projected and a detector function (e.g., network stack, network semblance) is evaluated for each candidate source, with the detector maximum corresponding to the most likely location. For FDTD calculations of travel-times we employed a UAS-derived Digital Elevation Model (DEM) of the SdF and the summit craters (Civico et al., 2024) areas conducted on the morning of 4 July with initial individual resolutions ranging between 20 and 50 cm/pixel. This DEM was merged with a basemap elevation model (Civico et al., 2021) of the rest of the island, re-sampled, and parsed into a 5x5 m grid for the purpose of FDTD modeling. For FDTD modeling, the source time function was approximated by a Blackman-Harris function with a cutoff frequency of 5 Hz (high enough to include the dominant frequency of the explosion signals while still allowing time-efficient computing) and the acoustic wavefield was propagated along the discretized topography using 15 grid points per wavelength (Wang, 1996). We used a constant sound velocity of 330 m s<sup>-1</sup> (estimated from the signal move-out across the network) and a stratified atmosphere model based on density and temperature data obtained from the Reanalysis v5 (ERA5) dataset (see Data and Resources), produced by the European Centre for Medium-Range Weather Forecasts of the Copernicus Climate Change Service. We used data corresponding to the ERA5 grid node closest to Stromboli, at 12:00 on 11, July 2024 (Coordinated Universal Time, UTC). The inferred source location for the paroxysmal explosion on 11, July 2024, along with a record section of the infrasound waveforms used and the detector function, are shown in Fig. 5. The location identifies a source located approximately 50m below the rim of the N crater (Fig. 5a) at an elevation of ~685 m. The estimated origin time for the event is 12:08:52 UTC.

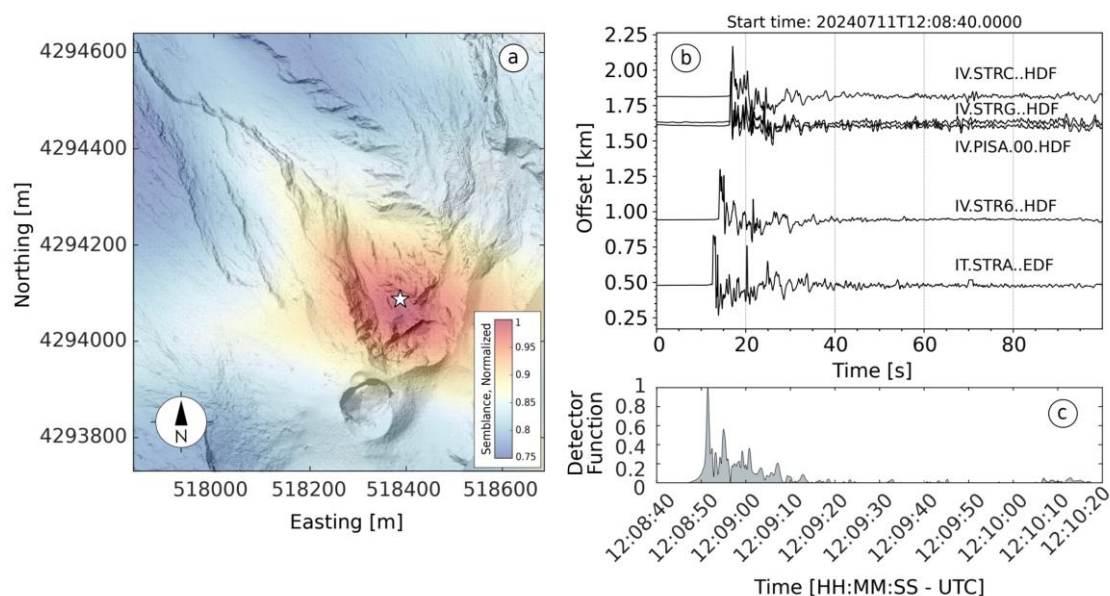


**Figure 5: Infrasound location of the 11 July, 2024 paroxysmal event using the RTM-FDTD method (see manuscript for details; DEM of July 14, 2024 from Civico et al. (2024)). a) Map-view of network semblance maximum around the Stromboli crater region. RTM-FDTD semblance location is indicated by a white star; b) record section of the filtered infrasound waveforms (bandpass filter 0.01-15 Hz) used for locating the event. The offset corresponds to source-station distance; c) Normalized network detector function (i.e., maximum network semblance amplitude over time).**

### 3.3 Deformation of unrest and eruptive events

Ground tilt at Stromboli has been frequently inferred to reflect processes like slug coalescence, slug ascent, and conduit emptying (Marchetti et al., 2009; Genco and Ripepe, 2010; Bonaccorso, 1998). Over the last decade, tilt has become central to real-time monitoring and eruption early warning at Stromboli. Ripepe et al. (2021a), for example, demonstrated the scale invariance of tilt at Stromboli, that is all explosions, regardless of their intensity, follow the same ground inflation-deflation pattern. A significant tilt was reported on 4 July (INGV-OE, 2024). The major explosion at 12:00 UTC was accompanied by a characteristic inflation-deflation pattern (Longo et al., 2024), followed by a pronounced deflation trend that began at 16:20 UTC and continued until 19:50 UTC (INGV-OE, 2024).

For the paroxysm on 11, July 2024 **fig. 5** shows the seismic-derived tilt, reconstructed from the EW horizontal component record at station STRE Aoyama et al. (2008), Genco and Ripepe (2010), and De Angelis and Bodin (2012). Slow inflation is observed, starting approximately 600 seconds before the explosion (Fig. 5b); the seismic-derived tilt sharply accelerates approximately 1 minute before reaching its peak of 1.5  $\mu$ rad at the onset of the explosion, followed by rapid deflation. This pattern is consistent with previous observations of tilt at Stromboli before paroxysms and major explosions (e.g. Genco and Ripepe (2010); Ripepe et al. (2021a)). We note that this tilt signal is derived from an individual seismic record, of an instrument





that is not likely oriented in the direction radial to the source; for this reason, we will focus on the interpretation of the deformation trend, and will not use the measured tilt amplitude for modelling purposes.

## 4 Discussion

In this manuscript we have presented geophysical data recorded between early and mid-July 2024 at Stromboli; the period of unrest included a major explosion on 4 July, significant collapse activity in the N summit crater area, emplacement of lava flows, and a paroxysmal event on 11 July. Surface activity at Stromboli intensified late in May with a marked increase in the occurrence of Strombolian explosions, the onset of effusive activity from SdF, and increasing volcanic tremor. Early in July, we observed a steady increase in volcanic tremor reaching unprecedented amplitudes on 4 July, (see Fig. 3a and Fig. 1S). Volcanic tremor at Stromboli has typically been linked to the coalescence of gas bubbles from layers of smaller bubbles and their ascent along the shallower conduit (McNutt et al., 2008; Chouet et al., 1997; Ripepe et al., 1999), suggesting that variations in tremor intensity are controlled by changes in gas flow within the conduit. It has been frequently speculated that an increase in volcanic tremor reflects an increase in the volume of gas within the magma (Ripepe et al., 1996), which in turn is linked to a higher occurrence of explosions at the top of the magma column. Field observations of increasing spattering in early July (Fig. 1) support a model of increased surface activity linked to the ascent of gas-rich magma within the shallow conduit. The high rates of VLP events observed during the same period further support the hypothesis of gas-rich magma migration within the shallow plumbing system. These events are traditionally associated with the rapid expansion of gas slugs rising through the liquid melt in the shallow conduit (Chouet et al., 2003; James et al., 2006); more recently (Ripepe et al., 2021) suggested that VLP waveforms at Stromboli are generated at the top of the magma column, mainly after the onset of Strombolian explosions; they showed that the occurrence of VLP event can be linked to explosive magma decompression in the uppermost ~ 250 m of the conduit. The recorded VLP events showed similar waveforms (Fig. 4b) suggesting a stable source mechanism and location; locations in the shallow parts of the conduit can be linked to magma accumulation at a shallow depth, close to the surface. While the number of VLP events did not show any significant variation before the major explosion on 4 July, volcanic tremor increased slowly but steadily (Fig. 3a). Coinciding with strong ground deflation after the major explosion (INGV-OE, 2024), volcanic tremor reached an unprecedented peak amplitude of  $\sim 8 \times 10^{-5}$  m s<sup>-1</sup> at ~17:00 UTC associated with the opening of a new effusive vent at ~ 510 m elevation within SdF (Fig. 2a) and the occurrence of numerous mass wasting events linked to collapse activity within the lower N crater area and upper section of SdF. We suggest that these signals reflect the emptying of the shallowest parts of the conduit system and the overall lowering of the magma level within the shallow volcano plumbing reflected in the opening of new effusive vents at progressively lower elevations. The transition between explosive and effusive regimes was also marked by a clear decrease in the occurrence of VLP events (Fig. 4), and a migration of their source deeper within the conduit (Ripepe et al., 2015). This contrasts with the flank eruptions of 2007 and 2014 (Ripepe et al., 2009; Ripepe et al., 2015) when VLP rates remained high during effusion; in July 2024 it appears that effusion reduced the overall explosivity, rather than recalling fresh magma from depth. The new effusive regime, indeed, was



262 characterized by a substantial lack of Strombolian explosive activity at the surface between 4-11 July, as observed in the field  
263 by our research team. The quasi-continuous collapse activity, observed from 13:00 UTC on 4, July, appeared to be linked to  
264 instabilities in the crater area around newly created vents; this instability persisted in the following days, with the number of  
265 events peaking on July 5 (83 recorded occurrences recorded in a single day (INGV-OE, 2024). The collapse activity recorded  
266 along the N crater rim, adjacent to the SdF, resulted in significant changes to the morphology of this sector of the volcanic  
267 edifice (Fig. 6).

268 During the study period, we also collected UAS data and compiled very high-resolution repeat DEMs (0.2-0.5 m/pixel), which  
269 allowed quantifying topographical changes via DEM differencing. The difference between DEMs on 4, July, (morning) and  
270 July 14 is shown in Fig. 7c. The data processing methodology follows the procedures described in Civico et al. (2022, 2024).  
271 The most notable morphological variations were observed in the afternoon of 4 July, while the paroxysm on 11 July did not  
272 lead to significant changes.

273 The summit craters were affected by loss of material due to the opening of two eruptive vents at approximately 700 and 500  
274 m a.s.l.. While the CS crater sector showed a roughly circular-shape crater floor deepening of about 84 m, the N sector was  
275 affected by the complete dismantling of its northern rim and external slope, marking the deepest morphological change  
276 occurred at the summit craters in the last decades, with a maximum difference in altitude of 109 m. The total volume loss  
277 recorded in the summit craters sector was estimated at 3.3 Mm<sup>3</sup> (Civico et al., 2024).

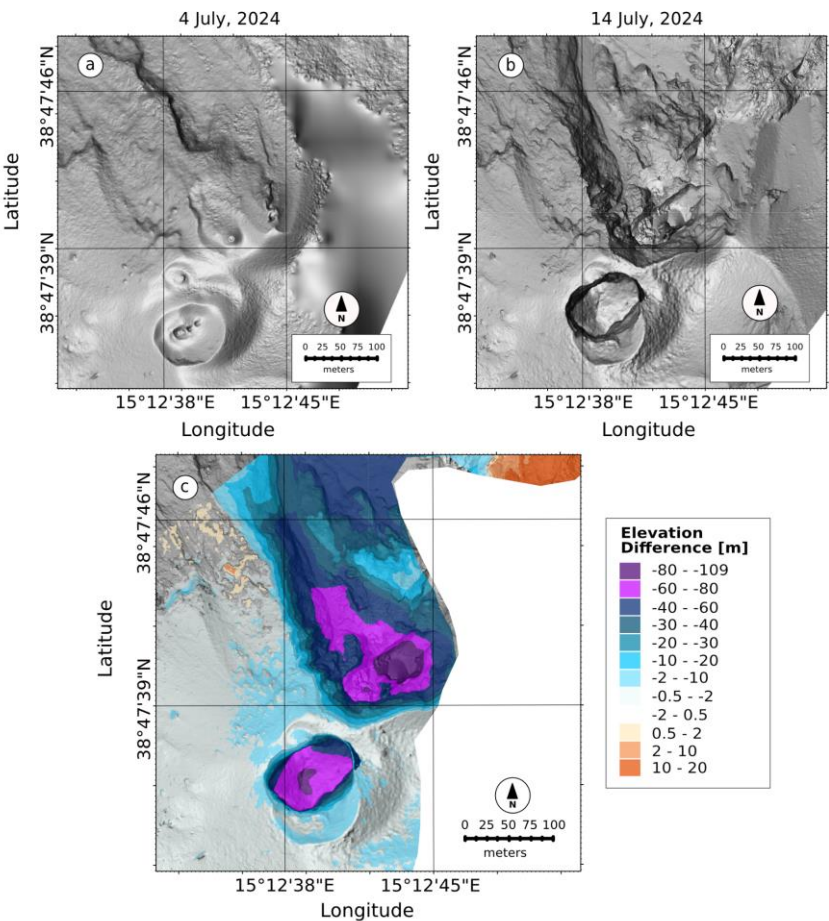


**Figure 6: Multidirectional hillshades of Stromboli's crater area: a) 4, July 2024 (Civico et al., 2024c), b) July 14, 2024 (Civico et al., 2024), c) map of elevation difference (Dem of Differences) highlighting morphological changes occurred between 4 and 14 July, 2024. Purple areas indicate material loss, whereas orange areas indicate material gain.**

Unlike the summit craters, the subaerial portion of the SdF slope was affected by both accumulation and erosion processes. Here, the main loss of material (2.74 Mm<sup>3</sup>; Civico et al., 2024a) was localized along the canyon formed in October 2022 (Di Traglia et al., 2024), which has widened and deepened during the July 2024 eruption. Accumulation processes instead were mainly due to PDC and lava flow deposits, localized in the northeastern sector of the slope. The maximum accumulation of lavas occurred at the new lava delta (maximum difference in altitude of 45 m), located in the center of the SdF shoreline. The effusive regime ended with the occurrence of the paroxysmal explosion on 11, July. The explosion generated an infrasonic pressure of 115 Pa at station STR6 with an associated VLP amplitude reaching  $5.8 \times 10^{-5} \text{ m s}^{-1}$  (see Fig. 3S). An ash plume reached a height of 5 km above the vent, and pyroclastic flows moved down the SdF. After that, volcanic activity reduced its intensity, showing low levels of tremor and VLP events although the tremor increased again on 12, July, associated with a small lava flow.



292 The eruptive crisis of July 2024, culminating in the paroxysm, is consistent with previous eruptions at Stromboli, such as those  
293 in April 2003, March 2007, and July-August 2019. The data discussed above can be used to inform a conceptual model of the  
294 entire sequence of processes responsible for the observed surface and eruptive activity, within the framework of previous  
295 studies (e.g., James et al., 2006; Chouet et al., 2008; Del Bello et al., 2012; Suckale et al., 2015; McKee et al., 2022).  
296 The spattering activity, observed at the start of our study period, represents an intensified form of puffing. Spattering activity  
297 results from the quasi-continuous bursting of small gas pockets within a bubbly flow regime, which generates pyroclasts  
298 fragments (Rosi et al., 2013). This activity typically marks the initial stages of unrest and eruption at Stromboli, where gas-  
299 rich magma is being actively degassed through continuous explosive bursts (Del Bello et al., 2012). At the more explosive end  
300 of the spectrum of Strombolian activity major explosions and paroxysms are often explained invoking the "slug model" (James  
301 et al., 2006; Chouet et al., 2008; Del Bello et al., 2012). In this model, gas bubbles (slugs) form deeper in the magma column  
302 and gradually coalesce as they rise through the conduit due to an increase of the magma viscosity. As gas slugs ascend, they  
303 expand due to decreasing pressure and eventually reach the surface. When they burst at the top of the magma column, they  
304 release gas explosively, fragmenting the magma and producing pyroclasts and feeding ash plumes of varying sizes. After the  
305 major explosion on 4 July, an effusive regime was established, characterized by lava flows, during which more degassed  
306 magma was erupted. Following the initial explosive activity driven by gas slugs, we infer that the transition to effusive regime  
307 is controlled by depressurization of the shallow plumbing system similar to Ripepe et al. (2017). The depressurization of the  
308 system caused by the initial explosive activity allowed magma to flow, and reach the surface forming lava flows, without  
309 further explosive activity. As the shallow volcanic conduit progressively emptied it leads to structural instability, causing  
310 collapses and landslides along the SdF.

311 According to Ripepe et al. (2017), the emptying of the conduit creates a vacuum effect that draws more gas-rich magma from  
312 deeper within the system. As volatile-rich magma rises and encounters lower pressures, it can lead to explosive eruptions,  
313 resulting in a paroxysmal event. The dynamics of the 11, July paroxysmal explosion displayed similar trends across seismic,  
314 acoustic, and deformation parameters compared to the others (Genco and Ripepe, 2010; Ripepe et al., 2021a). This consistency  
315 further validates the established models of Strombolian activity, where the largest explosions and energetic events, such as  
316 paroxysms, are driven by the same source mechanism. The scale-invariant conduit dynamics of ground deformation  
317 demonstrate that inflation amplitude and duration scale directly with the magnitude of the explosion (Ripepe et al., 2021a).  
318 Ground deformation observed on 11, July (Fig. 5) follows the same exponential inflation pattern as seen in previous paroxysms  
319 (Ripepe et al., 2021a). This behavior is typically explained by bubble dynamics, where the pressure on the conduit walls  
320 increases due to the rapid volumetric expansion of gas in highly vesiculated magma. As gas rises and expands, moreover, it  
321 pushes the magma column toward the surface, often leading to precursory lava emissions from the vent. Ground deformation  
322 is likely caused by a combination of increasing magma static pressure and the pressurization of degassed magma at the top of  
323 the column, driven by the exponential growth of gas. When the pressure applied by the gas-rich magma exceeds the tensile  
324 strength of the viscous magma plug, fragmentation occurs, resulting in the explosive release of gas and pyroclastic material  
325 (e.g. paroxysm). Another possible mechanism, proposed by Suckale et al. (2016) and McKee et al., (2022) suggests that the



explosion is triggered by the rapid expansion and release of gas when a partial rupture occurs in the plug at the top of the magma column.

## 5 Conclusion

The eruptive activity at Stromboli starting from 4, July, and culminating on 11, July 2024, with the paroxysm, provides a comprehensive case study of explosive volcanism at open-conduit volcanoes, thus offering additional insights and proofs for already existing source models.

The July 2024 paroxysm is preceded by a prolonged phase of heightened activity, characterized by increased volcanic tremor and VLP events. The high seismicity, combined with observed crater rim collapses and lava flows, suggests a progressive destabilization of the volcanic edifice. In particular, the major explosion on 4, July, and the subsequent paroxysm on 11, July highlight the role of magma gas dynamics, where increased gas volumes and pressure led to significant eruptive events.

Seismic analysis reveals that the volcanic tremor intensity is linked to gas-rich magma movement, reaching in this eruptive sequence unprecedented values at Stromboli. However, the variability in VLP events indicates that, while useful for monitoring overall volcano unrest, these signals alone may not serve as reliable precursors for major explosive events. Instead, the combined analysis of different geophysical parameters, including ground deformation, proved crucial for early warning and forecasting as previously suggested by Ripepe et al. (2021a).

Ground deformation patterns, specifically the inflation-deflation cycle observed before explosions, align with previous studies, confirming that such patterns reflect the occurrence of imminent explosions regardless of their magnitude. The exponential inflation observed before the paroxysm, caused by gas expansion and the rise of slugs within the magma column, is the same as in other paroxysmal events at Stromboli, supporting the already proposed source mechanism models for explosive events. Through UAS data, Civico et al. (2024) were able to estimate a total volume loss of about 6.0 Mm<sup>3</sup> involved after the gravitational mass collapses occurred on 4 and 11 July. The partial collapses generated a reshaping of the summit craters area as well as a deepening 2022 canyon along SdF, thus increasing the flank instability.

In conclusion, our results demonstrate how geophysical, visual observation and UAS-derived topographic data could offer valuable insights for tracking the volcanic explosive phenomena as well as the partial collapses of the summit craters due to the flank instability. This multiparametric monitoring approach could lead to significant advancements in reducing volcanic hazards at Stromboli.

## Data availability

The seismic waveform data from all the stations are part of INGV seismic network. The data are publicly available at EIDA Italia (<https://eida.ingv.it/>). The infrasound data are available upon request from the INGV- Osservatorio Vesuviano. The infrasonic collected from PISA station are available at <https://doi.org/10.5281/zenodo.14245572>.



356 **Author contribution**

357 L.Z., S.D.A. and P.S. wrote the proposals that funded installation and maintenance of the infrasound array and UAS, designed  
358 the field experiment, and financially supported this publication. L.Z. and S.D.A. tested the infrasonic equipment, organized  
359 fieldwork and participated in the original design of the experiment. L.Z., S.D.A., R.C., T.R. contributed to assembling the final  
360 multiparametric dataset and tested its quality and retrieval. L.Z., R.C. and T.R. installed and maintained the equipment during  
361 the field acquisition. L.Z., S.D.A. and D.G. performed analyses of infrasound data, seismic and tilt data, and prepared all  
362 figures. R.C. and T.R. analysed the UAS images. L.Z., D.G. and S.D.A. jointly wrote the initial draft of the manuscript and all  
363 authors contributed to review and edit the final version.

364 **Competing interests**

365 The authors declare that they have no conflict of interest.

366 **Acknowledgements**

367 INGV Project ‘Pianeta Dinamico (Dynamic Planet) - Working Earth’: Geosciences For The Understanding The Dynamics Of  
368 The Earth And The Consequent Natural Risks - “Dynamo - DYNAmics of eruptive phenoMena at basaltic vOlcanoes”  
369 (<https://progetti.ingv.it/it/pian-din/dynamo#project-info>).

370 INGV Departmental Strategic Project “UNO - UNderstanding the Ordinary to forecast the extraordinary: An integrated  
371 approach for studying and interpreting the explosive activity at Stromboli volcano” (<https://progetti.ingv.it/it/uno-stromboli>).

372 L.Z., D.G., S.D.A., R.C., T. R. and P.G. are supported by the grant “Progetto INGV Pianeta Dinamico” -Sub-project  
373 VT\_DYNAMO 2023- code CUP D53J19000170001 - funded by Italian Ministry MIUR (“Fondo Finalizzato al rilancio degli  
374 investimenti delle amministrazioni centrali dello Stato e allo sviluppo del Paese”, legge 145/2018).

375 We are indebted to all the INGV colleagues who have contributed to the monitoring efforts on Stromboli during July 2024 and  
376 the ones involved in the surveillance and network maintenance activities, to Maria Zagari (Italian Civil Aviation Authority -  
377 ENAC) for her help in issuing new NOTAMs during the emergency, and to Giuseppe De Rosa, Istituto Nazionale di  
378 Oceanografia e di Geofisica Sperimentale (OGS) for providing the photo of the 11, July paroxysm in Fig. 1.

379 The contents of this article represent the authors’ ideas and do not necessarily correspond to the official opinion and policies  
380 of the Dipartimento della Protezione Civile - Presidenza del Consiglio dei Ministri.e UAS images. We are grateful to the  
381 “Gruppo monitoring dell'Osservatorio Vesuviano” of INGV, Osservatorio Vesuviano (Italy), for their support in the data  
382 management.





### 383 **Financial support**

384 This work was supported by the grant "Progetto INGV Pianeta Dinamico" -Sub-project VT\_DYNAMO 2023- code CUP  
 385 D53J19000170001 - funded by Italian Ministry MIUR ("Fondo Finalizzato al rilancio degli investimenti delle amministrazioni  
 386 centrali dello Stato e allo sviluppo del Paese", legge 145/2018) and by NGV Departmental Strategic Project "UNO -  
 387 UNderstanding the Ordinary to forecast the extraordinary: An integrated approach for studying and interpreting the explosive  
 388 activity at Stromboli volcano".

### 389 **References**

- 390 Aiuppa, A., Burton, M., Caltabiano, T., Giudice, G., Guerrieri, S., Liuzzo, M., and Salerno, G.: Unusually large magmatic  
 391 CO<sub>2</sub> gas emissions prior to a basaltic paroxysm, *Geophys. Res. Lett.*, 37, <https://doi.org/10.1029/2010GL044997>, 2010.
- 392 Andronico, D., Del Bello, E., D'Oriano, C., Landi, P., Pardini, F., Scarlato, P., and Valentini, F.: Uncovering the eruptive  
 393 patterns of the 2019 double paroxysm eruption crisis of Stromboli volcano, *Nat. Commun.*, 12, [https://doi.org/10.1038/s41467-](https://doi.org/10.1038/s41467-021-23349-4)  
 394 021-23349-4, 2021.
- 395 Bertagnini, A., Métrich, N., Landi, P., and Rosi, M.: Stromboli volcano (Aeolian Archipelago, Italy): An open window on the  
 396 deep-feeding system of a steady state basaltic volcano, *J. Geophys. Res. Solid Earth*, 108,  
 397 <https://doi.org/10.1029/2002JB002146>, 2003.
- 398 Bonaccorso, A.: Evidence of a dyke-sheet intrusion at Stromboli Volcano inferred through continuous tilt, *Geophys. Res. Lett.*,  
 399 25, <https://doi.org/10.1029/98GL00766>, 1998.
- 400 Burton, M., Allard, P., Murè, F., and La Spina, A.: Magmatic gas composition reveals the source depth of slug-driven  
 401 Strombolian explosive activity, *Science*, 317, <https://doi.org/10.1126/science.1141900>, 2007.
- 402 Calvari, S., Spampinato, L., and Lodato, L.: The 5 April 2003 vulcanian paroxysmal explosion at Stromboli volcano (Italy)  
 403 from field observations and thermal data, *J. Volcanol. Geotherm. Res.*, 149, <https://doi.org/10.1016/j.jvolgeores.2005.09.008>,  
 404 2006.
- 405 Calvari, S., Spampinato, L., Bonaccorso, A., Oppenheimer, C., Rivalta, E., and Boschi, E.: Lava effusion—A slow fuse for  
 406 paroxysms at Stromboli volcano? *Earth Planet. Sci. Lett.*, <https://doi.org/10.1016/j.epsl.2011.03.005>, 2011.
- 407 Calvari, S., and Nunnari, G.: Statistical insights on the eruptive activity at Stromboli volcano (Italy) recorded from 1879 to  
 408 2023, *Remote Sensing*, 15, <https://doi.org/10.3390/rs15174298>, 2023.
- 409 Caricchi, L., Montagna, C. P., Aiuppa, A., Lages, J., Tamburello, G., and Papale, P.: CO<sub>2</sub> flushing triggers paroxysmal  
 410 eruptions at open conduit basaltic volcanoes, *J. Geophys. Res.: Solid Earth*, 129, <https://doi.org/10.1029/2023JB02561>, 2024.
- 411 Chouet, B., Saccorotti, G., Martini, M., Dawson, P., De Luca, G., Milana, G., and Scarpa, R.: Source and path effects in the  
 412 wave fields of tremor and explosions at Stromboli Volcano, Italy, *J. Geophys. Res.: Solid Earth*, 102,  
 413 <https://doi.org/10.1029/96JB03395>, 1997.





- 414 Chouet, B., Dawson, P., Ohminato, T., Martini, M., Saccorotti, G., Giudicepietro, F., De Luca, G., Milana, G., and Scarpa, R.:  
 415 Source mechanisms of explosions at Stromboli Volcano, Italy, determined from moment-tensor inversions of very-long-period  
 416 data, *J. Geophys. Res.: Solid Earth*, 108, <https://doi.org/10.1029/2002JB001919>, 2003.
- 417 Chouet, B., Dawson, P., and Martini, M.: Shallow-conduit dynamics at Stromboli Volcano, Italy, imaged from waveform  
 418 inversions, *Geol. Soc. London, Special Publications*, 307, <https://doi.org/10.1144/SP307.5>, 2008.
- 419 Colò, L., Ripepe, M., Baker, D. R., and Polacci, M.: Magma vesiculation and infrasonic activity at Stromboli open conduit  
 420 volcano, *Earth Planet. Sci. Lett.*, 292, <https://doi.org/10.1016/j.epsl.2010.01.041>, 2010.
- 421 Civico, R., Ricci, T., Scarlato, P., Andronico, D., Cantarero, M., Carr, B. B., De Beni, E., Del Bello, E., Johnson, J. B.,  
 422 Kueppers, U., Pizzimenti, L., Schmid, M., Strehlow, K., and Taddeucci, J.: Unoccupied Aircraft Systems (UASs) Reveal the  
 423 Morphological Changes at Stromboli Volcano (Italy) before, between, and after the 3 July and 28 August 2019 Paroxysmal  
 424 Eruptions, *Remote Sensing*, 13, <https://doi.org/10.3390/rs13010141>, 2021.
- 425 Civico, R., Ricci, T., Cecili, A., and Scarlato, P.: High-resolution topography reveals morphological changes of Stromboli  
 426 volcano following the July 2024 eruption, *Sci. Data*, 11, 1219, <https://doi.org/10.1038/s41597-024-04098-y>, 2024.
- 427 D'Auria, L., Giudicepietro, F., Martini, M., and Peluso, R.: Seismological insight into the kinematics of the 5 April 2003  
 428 vulcanian explosion at Stromboli volcano (southern Italy), *Geophys. Res. Lett.*, 33, <https://doi.org/10.1029/2005GL025502>,  
 429 2006.
- 430 De Angelis, S., and Bodin, P.: Watching the Wind: Seismic Data Contamination at Long Periods due to Atmospheric Pressure-  
 431 Field-Induced Tilting, *Bull. Seismol. Soc. Am.*, 102, <https://doi.org/10.1785/0120110245>, 2012.
- 432 Del Bello, E., Llewellyn, E. W., Taddeucci, J., Scarlato, P., and Lane, S. J.: An analytical model for gas overpressure in slug-  
 433 driven explosions: Insights into Strombolian volcanic eruptions, *J. Geophys. Res.: Solid Earth*, 117(B2),  
 434 <https://doi.org/10.1029/2011JB008747>, 2012.
- 435 Diaz-Moreno, A., Iezzi, A. M., Lamb, O. D., Fee, D., Kim, K., Zuccarello, L., and De Angelis, S.: Volume Flow Rate  
 436 Estimation for Small Explosions at Mt. Etna, Italy, From Acoustic Waveform Inversion, *Geophys. Res. Lett.*, 46,  
 437 <https://doi.org/10.1029/2019GL084159>, 2019.
- 438 Di Traglia, F., Berardino, P., Borselli, L., Calabria, P., Calvari, S., Casalbore, D., et al.: Generation of deposit-derived  
 439 pyroclastic density currents by repeated crater rim failures at Stromboli Volcano (Italy), *Bull. Volcanol.*, 86,  
 440 <https://doi.org/10.1007/s00445-024-01516-0>, 2024.
- 441 Delle Donne, D., Tamburello, G., Aiuppa, A., Bitetto, M., Lacanna, G., D'Aleo, R., and Ripepe, M.: Exploring the explosive-  
 442 effusive transition using permanent ultraviolet cameras, *J. Geophys. Res.: Solid Earth*, 122(6), 4377–4394,  
 443 <https://doi.org/10.1002/2017JB014027>, 2017.
- 444 European Centre for Medium-Range Weather Forecasts (ECMWF), ECMWF Reanalysis v5. Available at:  
 445 <https://www.ecmwf.int/en/forecasts/dataset/ecmwf-reanalysis-v5>. Access date: 21 July 2024.



446 Fee, D., Izbekov, P., Kim, K., Yokoo, A., Lopez, T., Prata, F., Kazahaya, R., Nakamichi, H., and Iguchi, M.: Eruption mass  
 447 estimation using infrasound waveform inversion and ash and gas measurements: Evaluation at Sakurajima Volcano, Japan,  
 448 *Earth Planet. Sci. Lett.*, 480, <https://doi.org/10.1016/j.epsl.2017.09.043>, 2017.

449 Fee, D., Toney, L., Kim, K., Sanderson, R. W., Iezzi, A. M., Matoza, R. S., De Angelis, S., Jolly, A. D., Lyons, J. J., and  
 450 Haney, M. M.: Local Explosion Detection and Infrasound Localization by Reverse Time Migration Using 3-D Finite-  
 451 Difference Wave Propagation, *Front. Earth Sci.*, 9, <https://doi.org/10.3389/feart.2021.640202>, 2021.

452 Francalanci, L., Tommasini, S., and Conticelli, S.: The volcanic activity of Stromboli in the 1906–1998 AD period:  
 453 mineralogical, geochemical and isotope data relevant to the understanding of the plumbing system, *J. Volcanol. Geotherm.*  
 454 *Res.*, 131, [https://doi.org/10.1016/S0377-0273\(03\)00364-1](https://doi.org/10.1016/S0377-0273(03)00364-1), 2004.

455 Francalanci, L., Davies, G. R., Lustenhouwer, W., Tommasini, S., Mason, P. R. D., and Conticelli, S.: Intra-Grain Sr Isotope  
 456 Evidence for Crystal Recycling and Multiple Magma Reservoirs in the Recent Activity of Stromboli Volcano, Southern Italy,  
 457 *J. Petrol.*, 46, <https://doi.org/10.1093/petrology/egi062>, 2005.

458 Genco, R., and Ripepe, M.: Inflation-deflation cycles revealed by tilt and seismic records at Stromboli volcano, *Geophys. Res.*  
 459 *Lett.*, 37, <https://doi.org/10.1029/2009GL042925>, 2010.

460 Giordano, G., and De Astis, G.: The summer 2019 basaltic Vulcanian eruptions (paroxysms) of Stromboli, *Bull. Volcanol.*,  
 461 83, <https://doi.org/10.1007/s00445-020-01403-0>, 2020.

462 Giudicepietro, F., Calvari, S., De Cesare, W., Di Lieto, B., Di Traglia, F., Esposito, A. M., Orazi, M., Romano, P., Tramelli,  
 463 A., Nolesini, T., Casagli, N., Calabria, P., and Macedonio, G.: Seismic and thermal precursors of crater collapses and overflows  
 464 at Stromboli volcano, *Sci. Rep.*, 13, <https://doi.org/10.1038/s41598-023-30198-9>, 2023.

465 Giudicepietro, F., López, C., Macedonio, G., Alparone, S., Bianco, F., Calvari, S., ... and Tramelli, A.: Geophysical precursors  
 466 of the July–August 2019 paroxysmal eruptive phase and their implications for Stromboli volcano (Italy) monitoring, *Sci. Rep.*,  
 467 10, 10296, <https://doi.org/10.1038/s41598-020-67160-w>, 2020.

468 Gheri, D., Zuccarello, L., De Angelis, S., Ricci, T., and Civico, R.: Infrasonic Data from the July 4–11, 2024 Paroxysm of  
 469 Stromboli Volcano [Data set]. Zenodo. <https://doi.org/10.5281/zenodo.14245572>, 2024.

470 Gurioli, L., Harris, A. J. L., Colò, L., Bernard, J., Favalli, M., Ripepe, M., and Andronico, D.: Classification, landing  
 471 distribution, and associated flight parameters for a bomb field emplaced during a single major explosion at Stromboli, Italy,  
 472 *Geology*, 41, <https://doi.org/10.1130/G33576.1>, 2013.

473 Harris, A., and Ripepe, M.: Temperature and dynamics of degassing at Stromboli, *J. Geophys. Res.: Solid Earth*, 112(B3),  
 474 <https://doi.org/10.1029/2006JB004393>, 2007.

475 INGV Bulletin of 25/06/2024: [https://www.ct.ingv.it/index.php/monitoraggio-e-sorveglianza/prodotti-del-](https://www.ct.ingv.it/index.php/monitoraggio-e-sorveglianza/prodotti-del-monitoraggio/bollettini-settimanali-multidisciplinari/914-bollettino-Settimanale-sul-monitoraggio-vulcanico-geochimico-e-sismico-del-vulcano-Stromboli-del-2024-06-25/file)  
 476 [monitoraggio/bollettini-settimanali-multidisciplinari/914-bollettino-Settimanale-sul-monitoraggio-vulcanico-geochimico-e-](https://www.ct.ingv.it/index.php/monitoraggio-e-sorveglianza/prodotti-del-monitoraggio/bollettini-settimanali-multidisciplinari/914-bollettino-Settimanale-sul-monitoraggio-vulcanico-geochimico-e-sismico-del-vulcano-Stromboli-del-2024-06-25/file)  
 477 [sismico-del-vulcano-Stromboli-del-2024-06-25/file](https://www.ct.ingv.it/index.php/monitoraggio-e-sorveglianza/prodotti-del-monitoraggio/bollettini-settimanali-multidisciplinari/914-bollettino-Settimanale-sul-monitoraggio-vulcanico-geochimico-e-sismico-del-vulcano-Stromboli-del-2024-06-25/file), last access: 19 August 2024.



- 478 INGV Bulletin of 02/07/2024: [https://www.ct.ingv.it/index.php/monitoraggio-e-sorveglianza/prodotti-del-](https://www.ct.ingv.it/index.php/monitoraggio-e-sorveglianza/prodotti-del-monitoraggio/bollettini-settimanali-multidisciplinari/915-bollettino-Settimanale-sul-monitoraggio-vulcanico-geochimico-e-sismico-del-vulcano-Stromboli-del-2024-07-02/file)  
 479 [monitoraggio/bollettini-settimanali-multidisciplinari/915-bollettino-Settimanale-sul-monitoraggio-vulcanico-geochimico-e-](https://www.ct.ingv.it/index.php/monitoraggio-e-sorveglianza/prodotti-del-monitoraggio/bollettini-settimanali-multidisciplinari/915-bollettino-Settimanale-sul-monitoraggio-vulcanico-geochimico-e-sismico-del-vulcano-Stromboli-del-2024-07-02/file)  
 480 [sismico-del-vulcano-Stromboli-del-2024-07-02/file](https://www.ct.ingv.it/index.php/monitoraggio-e-sorveglianza/prodotti-del-monitoraggio/bollettini-settimanali-multidisciplinari/915-bollettino-Settimanale-sul-monitoraggio-vulcanico-geochimico-e-sismico-del-vulcano-Stromboli-del-2024-07-02/file), last access: 19 August 2024.
- 481 INGV Bulletin of 09/07/2024: [https://www.ct.ingv.it/index.php/monitoraggio-e-sorveglianza/prodotti-del-](https://www.ct.ingv.it/index.php/monitoraggio-e-sorveglianza/prodotti-del-monitoraggio/bollettini-settimanali-multidisciplinari/918-bollettino-Settimanale-sul-monitoraggio-vulcanico-geochimico-e-sismico-del-vulcano-Stromboli-del-2024-07-09/file)  
 482 [monitoraggio/bollettini-settimanali-multidisciplinari/918-bollettino-Settimanale-sul-monitoraggio-vulcanico-geochimico-e-](https://www.ct.ingv.it/index.php/monitoraggio-e-sorveglianza/prodotti-del-monitoraggio/bollettini-settimanali-multidisciplinari/918-bollettino-Settimanale-sul-monitoraggio-vulcanico-geochimico-e-sismico-del-vulcano-Stromboli-del-2024-07-09/file)  
 483 [sismico-del-vulcano-Stromboli-del-2024-07-09/file](https://www.ct.ingv.it/index.php/monitoraggio-e-sorveglianza/prodotti-del-monitoraggio/bollettini-settimanali-multidisciplinari/918-bollettino-Settimanale-sul-monitoraggio-vulcanico-geochimico-e-sismico-del-vulcano-Stromboli-del-2024-07-09/file), last access: 19 August 2024.
- 484 INGV Bulletin of 16/07/2024: [https://www.ct.ingv.it/index.php/monitoraggio-e-sorveglianza/prodotti-del-](https://www.ct.ingv.it/index.php/monitoraggio-e-sorveglianza/prodotti-del-monitoraggio/bollettini-settimanali-multidisciplinari/920-bollettino-Settimanale-sul-monitoraggio-vulcanico-geochimico-e-sismico-del-vulcano-Stromboli-del-2024-07-16/file)  
 485 [monitoraggio/bollettini-settimanali-multidisciplinari/920-bollettino-Settimanale-sul-monitoraggio-vulcanico-geochimico-e-](https://www.ct.ingv.it/index.php/monitoraggio-e-sorveglianza/prodotti-del-monitoraggio/bollettini-settimanali-multidisciplinari/920-bollettino-Settimanale-sul-monitoraggio-vulcanico-geochimico-e-sismico-del-vulcano-Stromboli-del-2024-07-16/file)  
 486 [sismico-del-vulcano-Stromboli-del-2024-07-16/file](https://www.ct.ingv.it/index.php/monitoraggio-e-sorveglianza/prodotti-del-monitoraggio/bollettini-settimanali-multidisciplinari/920-bollettino-Settimanale-sul-monitoraggio-vulcanico-geochimico-e-sismico-del-vulcano-Stromboli-del-2024-07-16/file), last access: 19 August 2024.
- 487 James, M. R., Lane, S. J., and Chouet, B. A.: Gas slug ascent through changes in conduit diameter: Laboratory insights into a  
 488 volcano-seismic source process in low-viscosity magmas, *J. Geophys. Res.: Solid Earth*, 111,  
 489 <https://doi.org/10.1029/2005JB003718>, 2006.
- 490 Kim, K., and Lees, J. M.: Local Volcano Infrasound and Source Localization Investigated by 3D Simulation, *Seismol. Res. Lett.*, 85, <https://doi.org/10.1785/0220130135>, 2014.
- 492 Legrand, D., and Pertou, M.: What are VLP signals at Stromboli volcano? *J. Volcanol. Geotherm. Res.*, 421,  
 493 <https://doi.org/10.1016/j.jvolgeores.2021.107429>, 2022.
- 494 Longo, R., Lacanna, G., Innocenti, L., and Ripepe, M.: Artificial Intelligence and Machine Learning Tools for Improving Early  
 495 Warning Systems of Volcanic Eruptions: The Case of Stromboli, *IEEE Trans. Pattern Anal. Mach. Intell.*, 46(12), 7973–7982,  
 496 <https://doi.org/10.1109/TPAMI.2024.3399689>, 2024.
- 497 Marchetti, E., and Ripepe, M.: Stability of the seismic source during effusive and explosive activity at Stromboli Volcano,  
 498 *Geophys. Res. Lett.*, 32, <https://doi.org/10.1029/2005GL023962>, 2005.
- 499 Marchetti, E., Genco, R., and Ripepe, M.: Ground deformation and seismicity related to the propagation and drainage of the  
 500 dyke feeding system during the 2007 effusive eruption at Stromboli volcano (Italy), *J. Volcanol. Geotherm. Res.*, 182,  
 501 <https://doi.org/10.1016/j.jvolgeores.2009.01.029>, 2009.
- 502 McKee, K. F., Roman, D. C., Waite, G. P., and Fee, D.: Silent very long period seismic events (VLPs) at Stromboli Volcano,  
 503 Italy, *Geophys. Res. Lett.*, 49(23), e2022GL100735, <https://doi.org/10.1029/2022GL100735>, 2022.
- 504 McNutt, S. R., and Nishimura, T.: Volcanic tremor during eruptions: Temporal characteristics, scaling and constraints on  
 505 conduit size and processes, *J. Volcanol. Geotherm. Res.*, 178, <https://doi.org/10.1016/j.jvolgeores.2008.07.023>, 2008.
- 506 Pino, N. A., Moretti, R., Allard, P., and Boschi, E.: Seismic precursors of a basaltic paroxysmal explosion track deep gas  
 507 accumulation and slug upraise, *J. Geophys. Res.: Solid Earth*, 116, <https://doi.org/10.1029/2011JB008547>, 2011.
- 508 Pistolesi, M., Delle Donne, D., Pioli, L., Rosi, M., and Ripepe, M.: The 15 March 2007 explosive crisis at Stromboli volcano,  
 509 Italy: Assessing physical parameters through a multidisciplinary approach, *J. Geophys. Res.*, 116,  
 510 <https://doi.org/10.1029/2011JB008527>, 2011.



- 511 Ripepe, M.: Evidence for gas influence on volcanic seismic signals recorded at Stromboli, J. Volcanol. Geotherm. Res., 70,  
 512 [https://doi.org/10.1016/0377-0273\(96\)00033-8](https://doi.org/10.1016/0377-0273(96)00033-8), 1996a.
- 513 Ripepe, M., Poggi, P., Braun, T., and Gordeev, E.: Infrasonic waves and volcanic tremor at Stromboli, Geophys. Res. Lett.,  
 514 23, <https://doi.org/10.1029/96GL02394>, 1996b.
- 515 Ripepe, M., and Gordeev, E.: Gas bubble dynamics model for shallow volcanic tremor at Stromboli, J. Geophys. Res.: Solid  
 516 Earth, 104, <https://doi.org/10.1029/1998JB900046>, 1999.
- 517 Ripepe, M., Delle Donne, D., Lacanna, G., Marchetti, E., and Olivieri, G.: The onset of the 2007 Stromboli effusive eruption  
 518 recorded by an integrated geophysical network, J. Volcanol. Geotherm. Res., 182(3-4), 131–136,  
 519 <https://doi.org/10.1016/j.jvolgeores.2009.02.011>, 2009.
- 520 Ripepe, M., Delle Donne, D., Genco, R., Maggio, G., Pistolesi, M., Marchetti, E., Lacanna, G., Olivieri, G., and Poggi, P.:  
 521 Volcano seismicity and ground deformation unveil the gravity-driven magma discharge dynamics of a volcanic eruption, Nat.  
 522 Commun., 6(1), 6998, <https://doi.org/10.1038/ncomms7998>, 2015.
- 523 Ripepe, M., Pistolesi, M., Coppola, D., Delle Donne, D., Genco, R., Lacanna, G., ... and Valade, S.: Forecasting effusive  
 524 dynamics and decompression rates by magmastatic model at open-vent volcanoes, Sci. Rep., 7,  
 525 <https://doi.org/10.1038/s41598-017-00748-4>, 2017.
- 526 Ripepe, M., Lacanna, G., Pistolesi, M., Silengo, M. C., Aiuppa, A., Laiolo, M., ... and Delle Donne, D.: Ground deformation  
 527 reveals the scale-invariant conduit dynamics driving explosive basaltic eruptions, Nat. Commun., 12, 1683,  
 528 <https://doi.org/10.1038/s41467-021-21862-y>, 2021a.
- 529 Ripepe, M., Delle Donne, D., Legrand, D., Valade, S., and Lacanna, G.: Magma pressure discharge induces very long period  
 530 seismicity, Sci. Rep., 11, <https://doi.org/10.1038/s41598-021-86061-x>, 2021b.
- 531 Ripepe, M., and Lacanna, G.: Volcano generated tsunami recorded in the near source, Nat. Commun., 15,  
 532 <https://doi.org/10.1038/s41467-024-18567-x>, 2024.
- 533 Rizzo, A. L., Federico, C., Inguaggiato, S., Sollami, A., Tantillo, M., Vita, F., ... and Grassa, F.: The 2014 effusive eruption at  
 534 Stromboli volcano (Italy): Inferences from soil CO<sub>2</sub> flux and <sup>3</sup>He/<sup>4</sup>He ratio in thermal waters, Geophys. Res. Lett., 42,  
 535 <https://doi.org/10.1002/2015GL064152>, 2015.
- 536 Rosi, M., Bertagnini, A., Harris, A. J. L., Pioli, L., Pistolesi, M., and Ripepe, M.: A case history of paroxysmal explosion at  
 537 Stromboli: Timing and dynamics of the April 5, 2003 event, Earth Planet. Sci. Lett., 243,  
 538 <https://doi.org/10.1016/j.epsl.2006.01.035>, 2006.
- 539 Rosi, M., Pistolesi, M., Bertagnini, A., Landi, P., Pompilio, M., and Di Roberto, A.: Chapter 14 Stromboli volcano, Aeolian  
 540 Islands (Italy): present eruptive activity and hazards, Geol. Soc., London, Mem., 37, <https://doi.org/10.1144/M37.14>, 2013.
- 541 Sparks, R. S. J.: Dynamics of magma degassing, Geol. Soc., London, Spec. Publ., 213,  
 542 <https://doi.org/10.1144/GSL.SP.2003.213.01.07>, 2003.
- 543 Suckale, J., Keller, T., Cashman, K. V., and Persson, P.-O.: Flow-to-fracture transition in a volcanic mush plug may govern  
 544 normal eruptions at Stromboli, Geophys. Res. Lett., 43, <https://doi.org/10.1002/2016GL068082>, 2016.



- 545 Wang, S.: Finite-difference time-domain approach to underwater acoustic scattering problems, J. Acoust. Soc. Am., 99,  
546 <https://doi.org/10.1121/1.414620>, 1996.

# Geophysical fingerprint of the 4-11 July 2024 eruptive activity at Stromboli volcano, Italy.

Luciano Zuccarello<sup>1,2</sup>, Duccio Gheri<sup>1</sup>, Silvio De Angelis<sup>2,1</sup>, Riccardo Civico<sup>3</sup>, Tullio Ricci<sup>3</sup>, Piergiorgio Scarlato<sup>3</sup>.

<sup>1</sup>Istituto Nazionale di Geofisica e Vulcanologia, Sezione di Pisa, via Cesare Battisti, 53, 56125, Pisa, Italy.

<sup>2</sup>School of Environmental Sciences, University of Liverpool, 4 Brownlow Street, L69 3GP, Liverpool, UK.

<sup>3</sup>Istituto Nazionale di Geofisica e Vulcanologia, Sezione Roma 1, via di Vigna Murata, 605, 00143, Roma, Italy.

*Correspondence to:* Luciano Zuccarello (luciano.zuccarello@ingv.it); Duccio Gheri (duccio.gheri@ingv.it)

**Abstract.** Paroxysmal eruptions, characterized by sudden and vigorous explosive activity, are frequent at open-vent volcanoes. Stromboli volcano, Italy, is well-known for its nearly continuous degassing activity and mild explosions from the summit craters, occasionally punctuated by short-lived paroxysms. Here, we analyse multi-parameter geophysical data recorded at Stromboli in early July 2024, during a period of activity that led to a paroxysmal eruption on 11 July. We use seismic, infrasound and ground deformation data, complemented by visual and Unoccupied Aircraft System observations, to identify key geophysical precursors to the explosive activity and to reconstruct the sequence of events. Elevated levels of volcanic tremor and Very Long Period seismicity accompanied moderate explosive activity, lava emission and small collapses from the North crater, leading to a major explosion on 4 July, 2024 at 12:16 (UTC). Collapse activity from the North crater area continued throughout 7 July, while effusive activity occurred from two closely-spaced vents located within Sciara del Fuoco, on the Northwest flank of the volcano. On 11 July, a rapid increase in ground deformation preceded, by approximately 10 minutes, a paroxysmal event at 12:08 (UTC); the explosion produced a 5 km-high eruptive column and pyroclastic density currents along Sciara del Fuoco. Our observations suggest that the early activity in July was linked to eruption of resident magma within the shallowest parts of the volcano plumbing. This was followed by lowering of the magma level within the conduit system as confirmed by the location of newly opened effusive vents. Rapid ground deformation before the paroxysmal explosion on 11 July is consistent with the expansion of a gas-rich magma rising from depth, similar to past energetic explosive events at Stromboli. Our findings offer valuable insights into Stromboli's eruptive dynamics and other open-conduit volcanoes, highlighting the importance of integrated geophysical observations for understanding eruption dynamics, forecasting, and associated risk mitigation.

## 1 Introduction

Stromboli is an open conduit stratovolcano located in the Tyrrhenian Sea, off the northern coast of Sicily; its activity is characterized by continuous degassing and frequent, small-to-moderate, explosions occurring every few minutes from the summit craters, the well-known Strombolian activity. However, activity at Stromboli can rapidly escalate into more energetic

32 events, referred to as major explosions, which eject centimeter-to-meter-sized ballistic projectiles; at times, sustained explosive  
33 activity is accompanied by partial collapses of the crater rim (Gurioli et al., 2013; Di Traglia et al., 2024). Since 2019, major  
34 explosions at Stromboli have occurred with a frequency of about 4-5 events per year ejecting pyroclastic material to heights  
35 over a hundred meters, which can travel beyond the summit crater area and potentially affect tourist paths (Rosi et al., 2013;  
36 Gurioli et al., 2013). **During periods of** heightened activity, Stromboli may also experience paroxysms, that is highly energetic  
37 eruptions that generate eruptive columns exceeding 4 km in height, ballistics of up to 2 m in diameter and significant collapse  
38 activity from the summit crater areas (Fig. 1). Paroxysms can be accompanied by the emplacement of pyroclastic density  
39 currents (PDCs) along the Sciara del Fuoco (SdF, Fig. 1a), which can enter the sea and travel up to 2 km from the shoreline  
40 with demonstrated potential to trigger tsunamis (Rosi et al., 2006; Calvari et al., 2006; D'Auria et al., 2006; Ripepe and  
41 Lacanna, 2024). Although paroxysms are less frequent than major explosions, with an average occurrence of just one every  
42 four years since 2003, they are the most impactful hazard for the island of Stromboli (Rosi et al., 2013). **For instance, the** recent  
43 paroxysm **occurred** on 3 July, 2019, resulted in a fatality (Giudicepietro et al., 2020; Giordano and De Astis, 2020; Andronico  
44 et al., 2021).

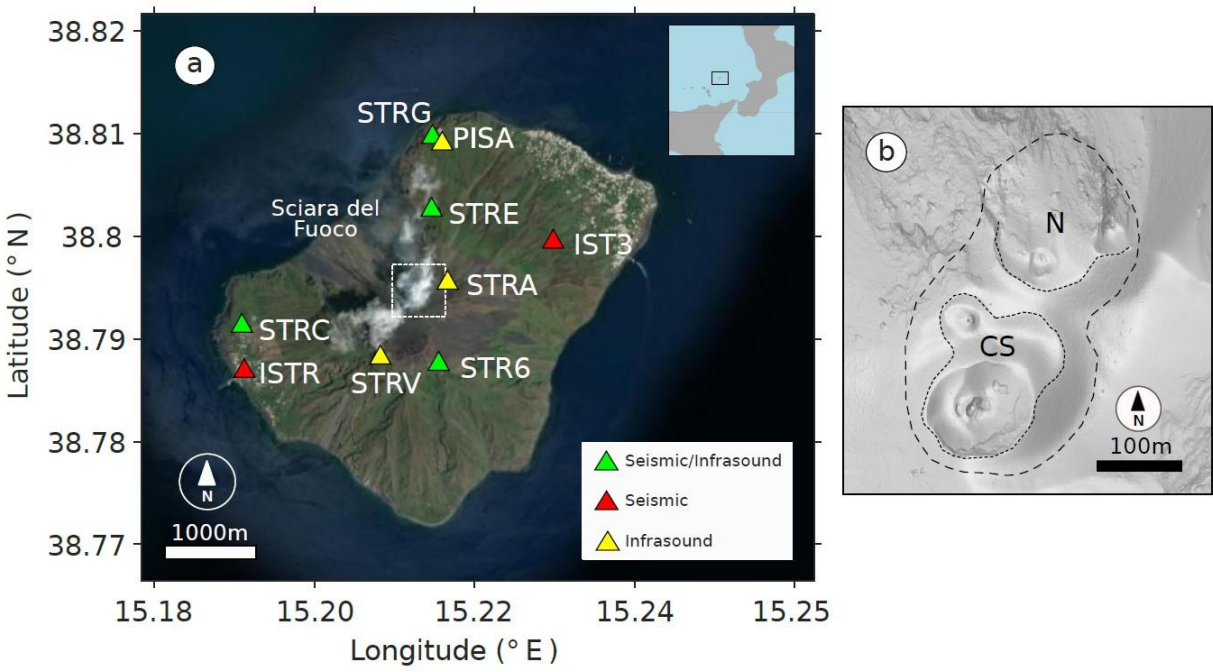
45 Unrest and eruption at Stromboli generate a broad range of geophysical signals. Nucleation and coalescence of gas bubbles  
46 into gas slugs (Sparks, 2003; Burton et al., 2007; Caricchi et al., 2024), and their ascent within the conduit generates  
47 characteristic seismic and deformation signals (Marchetti et al., 2009); gas slug bursting at the top of the magma column  
48 produces infrasound waves (Colò et al., 2010). Real-time detection and monitoring of these signals are crucial for risk  
49 mitigation at Stromboli, in the recent past, major explosions and paroxysms have been anticipated by detectable changes in  
50 geophysical signals between tens of seconds and minutes before their occurrence (Giudicepietro et al., 2020; Ripepe et al.,  
51 2021a; Longo et al., 2024). Except for the 2019 eruptive activity, the most intense in recent years, Stromboli's paroxysms are  
52 typically preceded by periods of lava effusion, or a general increase in surface activity that lasts for several days (Ripepe et  
53 al., 2009; Valade et al., 2016). Several studies have suggested that effusive eruptions may act as a trigger for paroxysmal  
54 explosions through a mechanism of decompression of the volcano plumbing system, evidenced by a drop in magma levels  
55 within the conduit (Aiuppa et al., 2010; Calvari et al., 2011; Ripepe et al., 2017). The most significant effusive event in terms  
56 of its volume occurred between December 2002 and July 2003 (Ripepe et al., 2017), which caused landslides, triggered a  
57 partial collapse of the SdF and culminated in a paroxysm on 5 April, 2003; this was the first large-scale paroxysmal event  
58 **recorded** since 1985 (Calvari and Nunnari, 2023). However, it should also be noted that effusive eruptions are not necessarily  
59 followed by paroxysms. An example is the November 2014 effusive eruption, which did not lead to paroxysmal activity (Rizzo  
60 et al., 2015). At the other end of the spectrum lies the paroxysm of July 2019, for which no clear increase in activity prior to  
61 the main event was recorded. As highlighted by Laiolo et al. (2022), thermal and gas flow levels had slightly increased but  
62 remained below "alert" thresholds.

63 Multi-parameter data are crucial to understand unrest at Stromboli and to detect transitions between low-to-moderate activity  
64 and more explosive phases (Pistolesi et al., 2011; Andronico et al., 2021). **A variety of models account for the occurrence and**  
65 **characteristics of seismic signal recorded at Stromboli and similar volcanoes (e.g., Chouet et al., 2008; Suckale et al., 2016;**



66 Ripepe et al., 2021b). Petrological analyses suggest Stromboli's conduit is stratified, with two types of magma: highly  
 67 porphyritic (HP) and low-porphyritic (LP) (Bertagnini et al., 2003; Francalanci et al., 2004, 2005). Eruptions are believed to  
 68 result from gas slugs rising through the HP magma, which acts as a viscous plug controlling their ascent and explosion (Sparks,  
 69 2003; Burton et al., 2007; Aiuppa et al., 2010; Caricchi et al., 2024). A recent model by Caricchi et al. (2024) suggests that  
 70 instability of gas-rich foam layers at the base of magma column could also trigger paroxysmal explosions.

71 In this study, we report on the most recent paroxysm at Stromboli, which occurred on 11 July, 2024, following a month of  
 72 unrest at the summit craters, as reported by the Istituto Nazionale di Geofisica e Vulcanologia (INGV) (INGV-OE, 2024). We  
 73 analyse the precursory geophysical activity leading up to the paroxysm based on seismic, infrasound and ground deformation  
 74 data gathered by the INGV monitoring network, complemented by observations conducted with Unoccupied Aircraft Systems  
 75 (UAS) during the study period. The UAS imagery provides a valuable tool to interpret geophysical data and understand the  
 76 conditions leading up to the paroxysm on 11 July, offering a high-resolution reconstruction of the eruptive events and  
 77 associated morphological changes at the volcano. Unless otherwise stated, all descriptions of surface activity in this manuscript  
 78 are from direct field observations by the authors during the study period.



79  
 80 **Figure 1: a) Map of monitoring network at Stromboli, showing the locations of seismo-acoustic, seismic, and infrasound sensors.**  
 81 **The inset shows the location of Stromboli volcano in Italy. b) Detail of the summit area of Stromboli, corresponding to the white**  
 82 **dash-line square in a), showing the North (N) and Center-South (CS) summit crater areas.**

## 83 2 Chronology of eruptive activity

84 The activity bulletins issued by INGV (see Data Availability), from 24 May until the early days of July, reported an increase  
85 in surface activity at Stromboli, particularly from the North (N) crater area (Fig. 1b), characterized by continuous and intense  
86 spattering, that is quasi-continuous emission of pyroclastic material through sequential, small-to-moderate, explosions ejecting  
87 ballistics at heights of ~10-20 m above the vent (Harris and Ripepe, 2007; Giudicedipietro et al., 2021) (Fig. 2a). The average  
88 frequency of explosions fluctuated between 13 (medium) and 16 (high) events/hour with spattering occasionally leading to  
89 lava flows along the SdF. On 23 and 28 June, lava flows began, following intense spattering from the N crater, converging  
90 into a canyon-like structure created by previous PDC activity in October 2022 (Di Traglia et al., 2024). Sulfur dioxide (SO<sub>2</sub>)  
91 and carbon dioxide (CO<sub>2</sub>) emissions remained at average levels, as did the carbon-to-sulfur (C/S) ratio (INGV-OE, 2024).  
92 On 3 July, at 16:35 UTC, intense spattering was observed from a vent located within the N crater sector, leading to a sequence  
93 of partial collapses of the N crater rim, which also remobilized material that had been erupted in the preceding days. These  
94 collapses mostly consisted of cold material with a minor contribution of hot deposits. At 17:02 UTC, a lava flow began from  
95 the same vent, accompanied by spattering and moderate explosions (Fig. 2b). The activity continued throughout the night, with  
96 lava fronts moving down to an elevation of 550-600 m a.s.l..  
97 On 4 July, at 12:11 UTC, a major explosion occurred from the N crater and, at 14:10 UTC, a new lava flow emerged at the  
98 base of the N crater area at ~700 m a.s.l., advancing towards Bastimento and Filo di Fuoco, located along the northeast  
99 boundary of SdF. After about one hour a second lava flow started at an elevation of ~580 m a.s.l., which reached the sea. At  
100 16:15 UTC, another vent opened at ~510 m a.s.l., producing a third lava flow accompanied by PDCs that rapidly descended  
101 the SdF into the sea (Fig. 2c). During the evening of 4 July, and throughout the following night, lava flow activity continued,  
102 accompanied by occasional collapses of pyroclastic materials.  
103 Between 5-6 July, 83 landslide events were observed, while effusive activity fluctuated and lava emission moved further  
104 downslope originating from two new eruptive vents at ~485 m a.s.l. (Fig. 2d). The flow formed a delta at the shoreline and  
105 steam plumes were observed caused by magma-seawater interaction. Explosive activity from the summit craters halted at the  
106 beginning of the effusive phase.  
107 On 11 July, at 12:08 UTC, a paroxysmal eruption occurred from the N crater area, producing an ash plume ~5 km high, which  
108 dispersed towards the southwest (Fig. 2e). Shortly after, a pyroclastic flow rapidly advanced along the SdF, which triggered a  
109 small-scale tsunami wave. The paroxysmal phase ended with a series of secondary and less intense PDCs.  
110 In the following hours, effusive activity ceased, and no further explosions were observed, except for a minor event on 12 July,  
111 at 08:28 UTC (Fig. 2a), which was followed by a small collapse event in the N crater area.

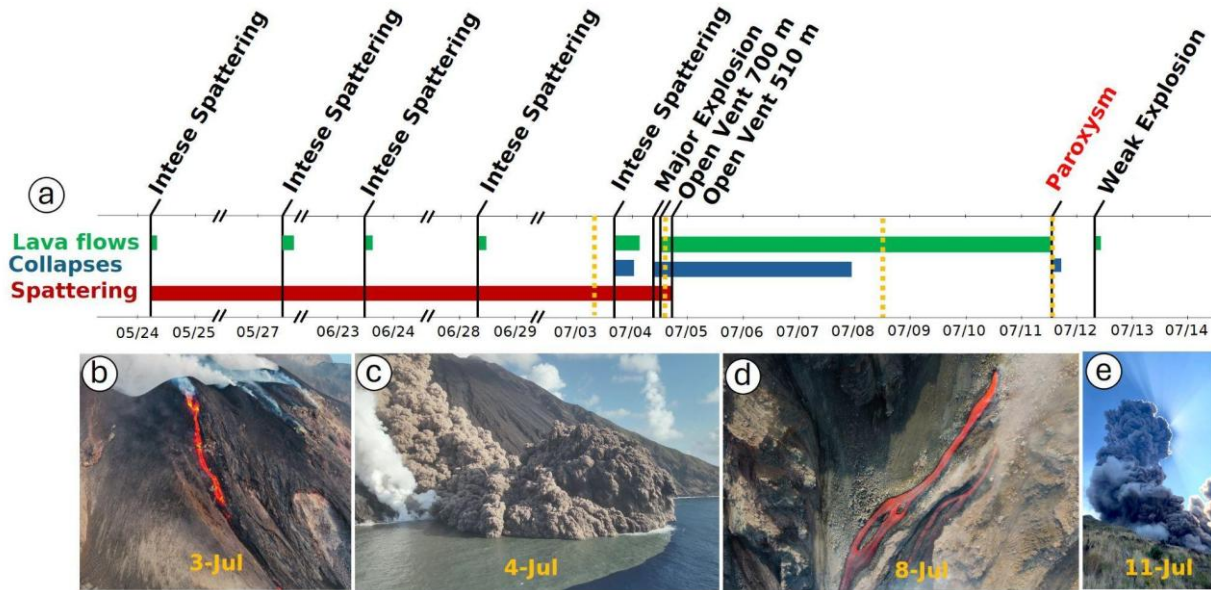


**Figure 2: Timeline of the observed surface activity and key visual observations at Stromboli between late May and mid-July, 2024.**  
a) Timeline showing the chronology of activity, which marks periods of activity characterized by lava flows (green), collapses (blue) and spattering (red). Significant events are labelled, such as intense spattering, a major explosion on 4 July, opening of new vents, and the paroxysm on 11 July. b-e) Sequence of images gathered at the times indicated by the dashed yellow lines in a). From left to right: spattering activity on 3 July, a PDC event reaching into the sea on 4 July, continued lava flow on 8 July, and the paroxysmal explosion on 11 July (photo “e” courtesy of G. De Rosa - OGS).

### 3 Geophysical observations

In this study we use data recorded by the geophysical monitoring network deployed and maintained on Stromboli by INGV (Fig. 1a). The network includes two seismic broadband stations, equipped with Nanometrics Trillium (0.02–40 s) 3-component seismometers and Trident digital acquisition systems (IST3 and ISTR stations), as well as other four broadband station employing two GURALP CMG-3ESPC 120 s and two GURALP CMG-40T-60S seismometers (STR6 - STRE and STRC-STRG respectively). All the data recorded are digitized at 100 Hz.

The infrasound network includes five Chaparral microphones at the stations STRA, STRC, STRG, STRE and STR6, and a Geco srl sensor at STRV. Infrasound data are digitized at 100Hz (only STRA at 50 Hz) and recorded with 24-bit resolution using Guralp Affinity and Gaia2 digitizers (<https://eida.ingv.it/>; <https://www.ov.ingv.it/index.php/ricercanew/stromboli>). An additional infrasound station, called PISA (Fig. 1a), was deployed on 4 July at 13:35 UTC, 35 minutes before the onset of the effusive activity. Pisa was equipped with an IST-2018 broadband microphone, and the data were sampled at 100 Hz using DIGOS DATA-CUBE<sup>3</sup> 24-bit digitizer (e.g., Gheri et al., 2024).

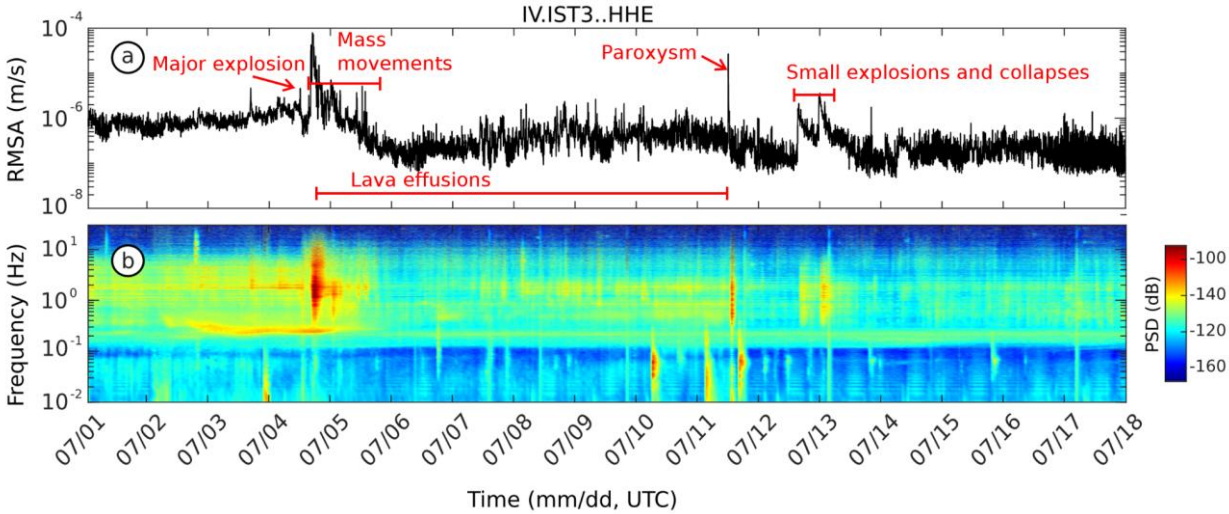
### 132 3.1 Seismic characterization of eruptive events

133 Volcanic tremor is traditionally thought to reflect magma movement within the conduit (McNutt and Nishimura, 2008; Chouet  
134 et al., 1997; Ripepe and Gordeev, 1999); at Stromboli, **volcanic** tremor is routinely monitored by means of the Root Mean  
135 Square (RMS) of the continuous seismic signal (**5-minut moving window**) in the 1-3 Hz frequency band (Giudicepietro et al.,  
136 2023). Figure 3a shows RMS **tremor amplitude values** of the order of  $10^{-6} \text{ ms}^{-1}$  (recorded at the **IST3** site), which correspond  
137 to tremor classified by INGV as high. A marked and short-lived increase in seismic RMS **tremor amplitude** was observed after  
138 the major explosion at 12:11 on 4 July (Fig. 3a). During this period, the signal reached unprecedented levels, peaking at  $10^{-4}$   
139  $\text{ms}^{-1}$  at 17:00 UTC. Short-lived increases in RMS **tremor amplitude** values were still noted throughout 5 July, although the  
140 **RMS** exhibited an overall decline to values of the order of  $10^{-7} \text{ ms}^{-1}$ , lower than those recorded at the beginning of July. In the  
141 following days (6-11 July), the **RMS tremor amplitude** was marked by a series of short-duration peaks during lava flow activity.  
142 This behaviour changed again on 11 July, when the onset of paroxysmal activity coincided with a new increase in RMS **tremor**  
143 **amplitude** (Fig. 3a). After the paroxysm, the RMS **tremor amplitude** decreased again with only sparse and brief intervals of  
144 increased amplitudes between 12-13 July (Fig. 3a). From late 13 July, onwards, the amplitude stabilized around  $10^{-7} \text{ ms}^{-1}$ ,  
145 indicating that volcanic activity had reduced and returned to background levels. Additional details of the signals recorded on  
146 4-11 July, are shown in the Supplementary Materials (Fig. 1Sa).

147 The spectrogram in Fig. 3b shows nearly continuous energy in the 1-3 Hz range, typically associated with tremor signals at  
148 Stromboli (Ripepe et al., 1996). Energy levels in this band change throughout the pre-, syn-, and post-explosive activity  
149 periods, **peaking on 4 July (dark red in Fig. 3b) at 17:15 UTC, following the major explosion, which coincides with the RMS**  
150 **peak (see also Fig. 1Sce)**. A pulsating phase was observed from 6-11 July, with another peak during the paroxysm. Explosive  
151 activity between 4-11 July, exhibited a broader frequency range in the 0.5-15 Hz band. It is worth noting that the eruptive  
152 event on 4~~7~~ July was preceded by a high-energy signal in the narrow frequency band 0.2-0.3 Hz (Fig. 3b). We also observe  
153 that this very low-frequency signal was not recorded before the paroxysm on 11, July. Finally, on **10 July** at 05:09 UTC and  
154 on 11 July at 02:26 and 15:21 UTC, high-energy signals were observed around 0.05-0.08 Hz, exhibiting a dispersive spectrum  
155 typical of teleseismic events as reported by USGS (for further information, see:  
156 <https://earthquake.usgs.gov/earthquakes/search/>).

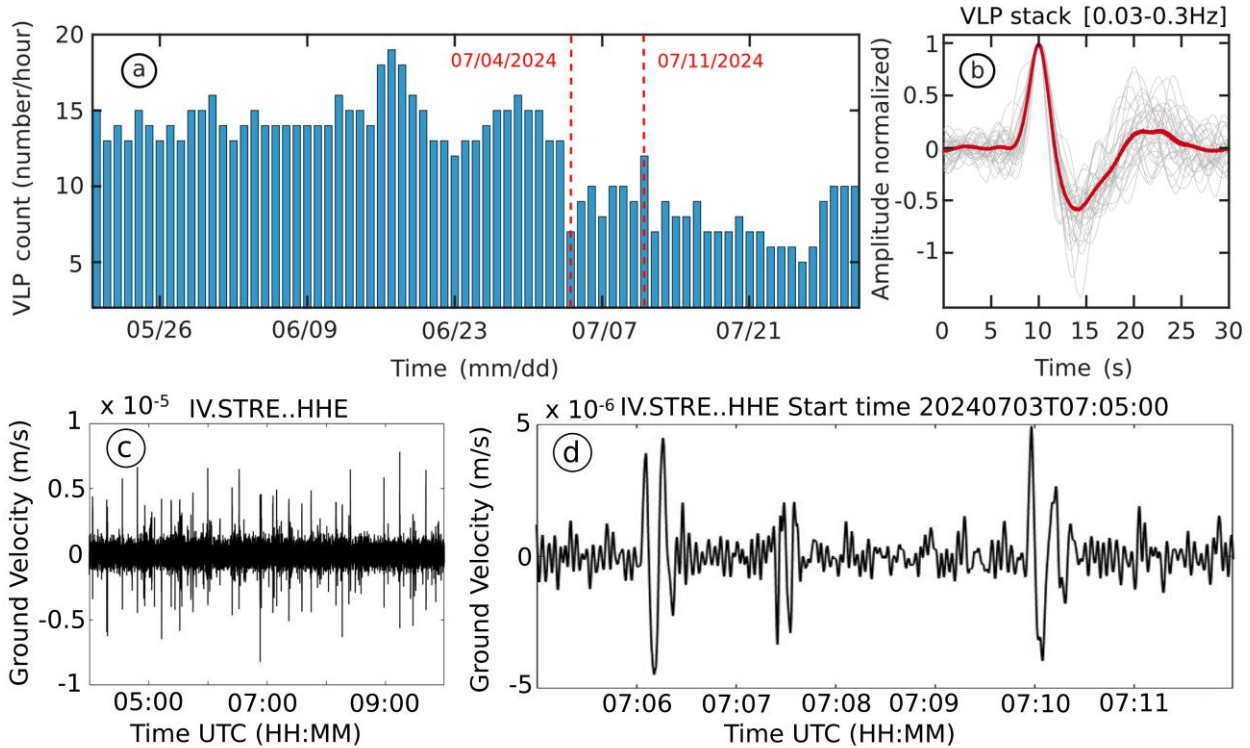
157 We have also analysed the occurrence of Very Long Period (VLP) earthquakes that have traditionally been associated with  
158 pressure disturbances and the dynamics of gas-rich magma within fluid-filled structures (Chouet et al., 1997; Chouet et al.,  
159 1999; Marchetti and Ripepe, 2005; Legrand and Perton, 2022), and one of the main tools used to monitor unrest at Stromboli.  
160 **VLP events at Stromboli are thought to be generated by a pre-eruptive expansion due to rising pressure in the magma column,**  
161 **followed by a post-eruptive contraction as pressure decreases. Final oscillations in the VLP signal may be caused by**  
162 **fluctuations in the conduit or edifice. (Legrand and Perton, 2022)**. An increase in the frequency of occurrence of these signals  
163 is typically a precursor to periods of elevated eruptive activity (Ripepe et al 2009; Delle Donne et al., 2017). Figure 4a derived  
164 from information sourced from the INGV bulletins (INGV-OE, 2024), provides an overview of the rates of VLP seismicity at

165 Stromboli between the end of May and mid-July 2024, after the 11 July paroxysm. From May until mid-June, VLP event rates  
 166 remained stable, fluctuating around high values between 12 and 15 events/hour. A mean rate of ~13 events/hour is defined, at  
 167 Stromboli, as “normal activity” (Ripepe et al., 2008) and it suggests that an efficient degassing mechanism of the magma  
 168 column is established (Ripepe et al., 2021b). A significant peak is observed around mid-June, with the number of VLP events  
 169 reaching 19 events/hour on June 16. This peak is followed by a slight decrease in event rates, although the number of events  
 170 remained elevated compared to previous days. Figure 4b shows the characteristic compression-decompression cycle of VLP  
 171 events at Stromboli; this waveform represents the normalized stack of all VLP events with maximum amplitude greater than  
 172  $5 \times 10^{-6} \text{ ms}^{-1}$  at station STRE. Figure 4c, and more specifically 4d, shows a 1-day filtered (0.03-0.3Hz) seismic record  
 173 illustrating the occurrence of VLP events as recorded at station STRE, the closest seismo-acoustic station to the eruptive area,  
 174 located on the east flank of SdF at 495 m of elevation (see Fig. 1).  
 175 Before the major explosion on 4 July, we observed a clear drop in the occurrence of VLP events (Fig. 4a) from 10-15 to 7-10  
 176 events/hour. The rates of VLP events remained stable until the 11 July paroxysm, peaking again at 12 events/hour on that day.  
 177 After the paroxysm, a further decrease in VLP rates was observed with hourly counts ranging from 6 to 10 events.



178  
 179 **Figure 3: a) Seismic tremor or RMS tremor amplitude** calculated every minute using a moving time window of 5 minutes, within  
 180 the volcanic tremor frequency band of Stromboli (1-3 Hz), from 2 to 18 July. b) Spectrogram of the E-component from the IST3  
 181 seismic station for the same period.





182

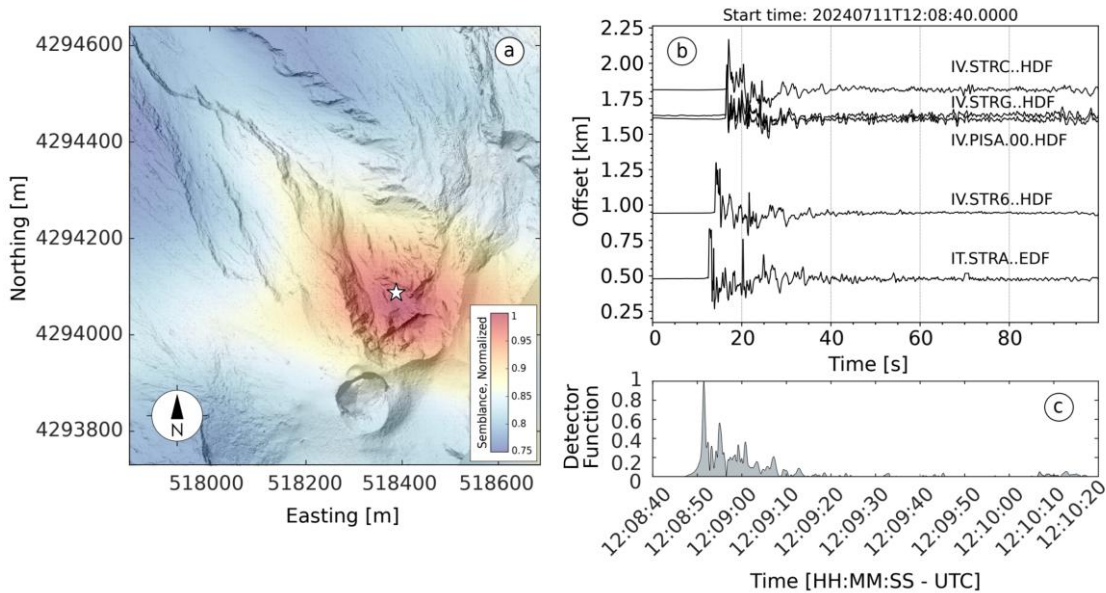
183 **Figure 4: a) Hourly rates of VLP events from the INGV catalog. Vertical red dashed lines indicate the major explosion and paroxysm**  
 184 **that occurred on 4 and 11 July, respectively. b) VLP waveform events ( $>5 \times 10^{-6} \text{ ms}^{-1}$ ) recorded on 3 July, at station STRE normalized**  
 185 **with respect to maximum amplitude (light grey). The red waveform represents the average of all high-amplitude waveforms. c)**  
 186 **Continuous waveform recorded at station STRE (EW component) on 3 July 2024, filtered between 0.03-0.3 Hz. d) Extract from c)**  
 187 **showing a sequence of VLP events recorded on 3 July over a 7-minute period by the STRE station on the same horizontal component**

### 188 3.2 Infrasound location of the 11 July, 2024 paroxysm

189 We have also analysed infrasound data recorded by the INGV acoustic monitoring network and an additional microphone  
 190 installed during the period of activity (Fig. 1). The infrasonic record before 4 July, shows a typical background of moderate  
 191 strombolian activity occasionally interspersed with larger explosions (see Fig. 2Sa). The major explosion on 4 July, generated  
 192 an infrasonic transient with a pressure of 5 Pa (Fig. 2Sb) at station STR6, **~750m from the CS crater area**. Following this event,  
 193 a marked decrease in acoustic energy was observed until the 11 July paroxysmal event, which produced infrasonic waves with  
 194 a peak amplitude of 115 Pa at the STR6 site (at **~750 m from the source**; see Fig. 1a and Fig. 2Sc).

195 **By analysing infrasound data, we located** the source of the paroxysmal eruption on 11 July, 2024. We employed the RTM-  
 196 FDTD (Reverse Time Migration - Finite Difference Time Domain) method of Fee et al. (2021), which implements waveform  
 197 back-projection over a grid of candidate source locations. Travel-times between potential source locations and all stations in  
 198 the network are calculated via FDTD modeling (Kim and Lees, 2014; Fee et al., 2017; Diaz-Moreno et al., 2019) to account  
 199 for the effect of topography on the propagation of the acoustic wavefield. In the RTM-FDTD method, waveforms are back-

200 projected and a detector function (e.g., network stack, network semblance) is evaluated for each candidate source, with the  
 201 detector maximum corresponding to the most likely location. For FDTD calculations of travel-times we employed a UAS-  
 202 derived Digital Elevation Model (DEM) of the SdF and the summit craters (Civico et al., 2024ab) areas conducted on the  
 203 morning of 4 July with initial individual resolutions ranging between 20 and 50 cm/pixel. This DEM was merged with a  
 204 reference elevation model (Civico et al., 2021) of the rest of the island, re-sampled, and parsed into a 5x5 m grid for the purpose  
 205 of FDTD modeling. For FDTD modeling, the source time function was approximated by a Blackman-Harris function with a  
 206 cutoff frequency of 5 Hz (high enough to include the dominant frequency of the explosion signals, between 0.2 and 2 Hz,  
 207 while still allowing time-efficient computing) and the acoustic wavefield was propagated along the discretized topography  
 208 using 15 grid points per wavelength (Wang, 1996). We used a constant sound velocity of 330 ms<sup>-1</sup> (estimated from the signal  
 209 move-out across the network) and a stratified atmosphere model based on density and temperature data obtained from the  
 210 Reanalysis v5 (ERA5) dataset (see Data and Resources), produced by the European Centre for Medium-Range Weather  
 211 Forecasts of the Copernicus Climate Change Service. We used data corresponding to the ERA5 grid node closest to Stromboli,  
 212 at 12:00 on 11 July, 2024 (Coordinated Universal Time, UTC). The inferred source location for the paroxysmal explosion on  
 213 11 July, 2024, along with a record section of the infrasound waveforms used and the detector function, are shown in Fig. 5.  
 214 The location identifies a source located approximately 50m below the rim of the N crater (Fig. 5a) at an elevation of ~685 m.  
 215 The estimated origin time for the event is 12:08:52 UTC.



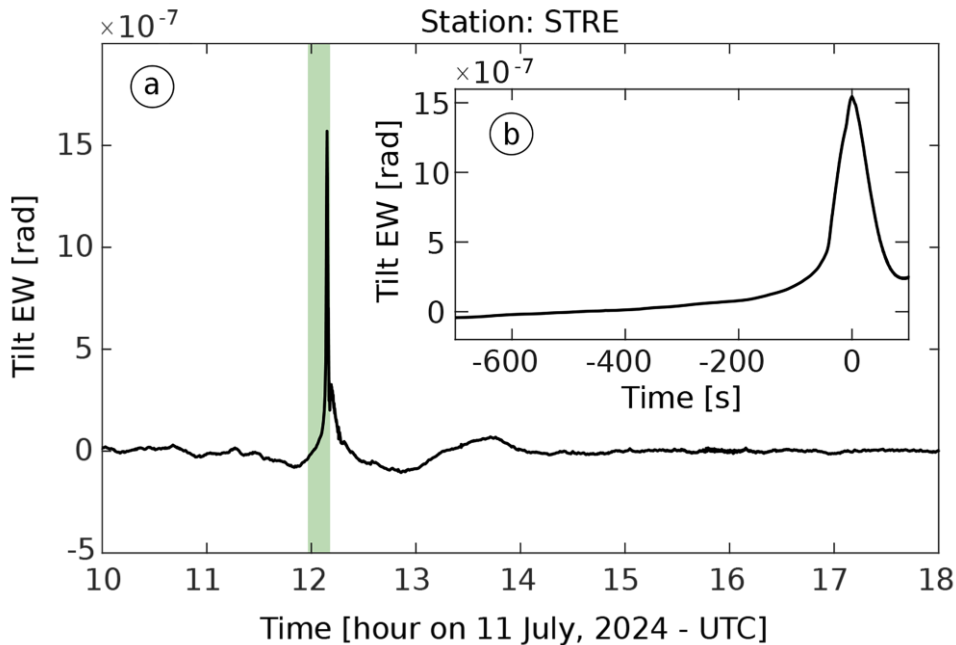
216  
 217 **Figure 5: Infrasound location of the 11 July, 2024 paroxysmal event using the RTM-FDTD method (see manuscript for details; DEM**  
 218 **of 14 July, 2024 from Civico et al. (2024a,b). a) Map-view of network semblance maximum around the Stromboli crater region.**  
 219 **RTM-FDTD semblance location is indicated by a white star; b) record section of the filtered infrasound waveforms (bandpass filter**  
 220 **0.01-15Hz) used for locating the event. The offset corresponds to source-station distance; c) Normalized network detector function**  
 221 **(i.e., maximum network semblance amplitude over time).**



222 **3.3 Tilt and eruptive events**

223 Ground tilt at Stromboli has frequently been inferred to reflect processes like slug coalescence, slug ascent, and conduit  
224 emptying (Marchetti et al., 2009; Genco and Ripepe, 2010; Bonaccorso, 1998). Over the last decade, tilt has become central  
225 to real-time monitoring and eruption early warning at Stromboli. Ripepe et al. (2021a), for example, demonstrated the scale  
226 invariance of tilt at Stromboli, that is all explosions, regardless of their intensity, follow the same ground inflation-deflation  
227 pattern. A significant tilt was reported on 4 July (INGV-OE, 2024). The major explosion at 12:00 UTC was accompanied by  
228 a characteristic inflation-deflation pattern (Longo et al., 2024), followed by a pronounced deflation trend that began at 16:20  
229 UTC and continued until 19:50 UTC (INGV-OE, 2024).

230



231 **Figure 6: a) Radial tilt recorded by STRE broadband seismic station on 11 July, 2024; b) detail of tilt recorded before the 11 July**  
232 **paroxysm: the signal shows a marked amplitude increases starting ~10 minutes before the onset of the explosion.**  
233  
234  
235 For the paroxysm on 11 July, 2024 Fig. 6 shows the seismic-derived tilt, reconstructed from the EW horizontal component  
236 record at station STRE. The relationship between displacement and tilt sensitivity is a function of the long-period corner  
237 frequency of the seismometer used. By applying a magnification factor (e.g., Aoyama et al. (2008), Genco and Ripepe (2010),  
238 and De Angelis and Bodin (2012)), which is constant around the natural period of the seismometer, we were able to convert  
239 the seismometer's output from displacement to ground tilt. Slow inflation is observed, starting ~600 seconds before the  
240 explosion (Fig. 6b); the seismic-derived tilt sharply accelerates approximately 1 minute before reaching its peak of 1.5  $\mu$ rad at  
241 the onset of the explosion, followed by rapid deflation. This pattern is consistent with previous observations of tilt at Stromboli  
242 before paroxysms and major explosions (e.g. Genco and Ripepe (2010); Ripepe et al. (2021a)). We note that this tilt signal is

243 derived from an individual seismic record, of an instrument that is not likely oriented in the direction radial to the source; for  
244 this reason, we will focus on the interpretation of the deformation trend and will not use the measured tilt amplitude for  
245 modelling purposes.

## 246 **4 Discussion**

247 In this manuscript we have presented geophysical data recorded between early and mid-July 2024 at Stromboli; the period of  
248 unrest included a major explosion on 4 July, significant collapse activity in the N summit crater area, emplacement of lava  
249 flows, and a paroxysmal event on 11 July. Surface activity at Stromboli intensified late in May with a marked increase in the  
250 occurrence of Strombolian explosions, the onset of effusive activity from SdF, and increasing volcanic tremor. **Using multi-**  
251 **parameter observations, we reconstructed the chronology of the eruptive activity, which culminated in the paroxysmal**  
252 **explosion on 11 July, 2024.**

253

### 254 **4.1 Eruptive activity during the first week of July, 2024.**

255 **In the first week of July**, we observed a steady increase in volcanic tremor reaching unprecedented amplitudes on 4 July, (see  
256 Fig. 3a and Fig. 1S). Volcanic tremor at Stromboli has typically been linked to the coalescence of gas bubbles from layers of  
257 smaller bubbles and their ascent along the shallower conduit (McNutt et al., 2008; Chouet et al., 1997; Ripepe et al., 1999),  
258 suggesting that variations in tremor intensity are controlled by changes in gas flow within the conduit.

259 It has been frequently speculated that an increase in volcanic tremor reflects an increase in the volume of gas within the magma  
260 (Ripepe et al., 1996), which in turn is linked to a higher occurrence of explosions at the top of the magma column. Field  
261 observations of increasing spattering in early July (Fig. 1) support a model of increased surface activity linked to the ascent of  
262 gas-rich magma within the shallow conduit. **The spattering activity observed at the start of our study period, represents an**  
263 **intensified form of puffing. Spattering results from the quasi-continuous bursting of small gas pockets within a bubbly flow**  
264 **regime, which generates pyroclasts (Rosi et al., 2013). This activity typically marks the initial stages of unrest and eruption at**  
265 **Stromboli, where gas-rich magma is actively degassed through continuous explosive bursts (Del Bello et al., 2012).** The high  
266 rates of VLP events observed during the same period further support the hypothesis of gas-rich magma migration within the  
267 shallow plumbing system. These events are traditionally **linked to** the rapid expansion of gas **bubbles** rising through the liquid  
268 melt in the shallow conduit (Chouet et al., 2003; James et al., 2006); more recently Ripepe et al.(2021) suggested that VLP  
269 waveforms at Stromboli are generated at the top of the magma column, mainly after the onset of Strombolian explosions; they  
270 showed that the occurrence of VLP event can be linked to explosive magma decompression in the uppermost ~ 250 m of the  
271 conduit. The recorded VLP events showed similar waveforms (Fig. 4b) suggesting a stable source mechanism and location;  
272 locations in the shallow parts of the conduit can be linked to magma accumulation at a shallow depth, close to the surface.  
273 While the number of VLP events did not show any significant variation before the major explosion on 4 July, volcanic tremor  
274 increased slowly but steadily (Fig. 3a). Coinciding with strong ground deflation after the major explosion (INGV-OE, 2024),

275 volcanic tremor reached an unprecedented peak amplitude of  $\sim 8 \times 10^{-5} \text{ ms}^{-1}$  at  $\sim 17:00$  UTC associated with the opening of a  
276 new effusive vent at  $\sim 510$  m elevation within SdF (Fig. 2a) and the occurrence of numerous mass wasting events linked to  
277 collapse activity within the lower N crater area and upper section of SdF. We suggest that these signals reflect the emptying  
278 of the shallowest parts of the conduit system and the overall lowering of the magma level within the shallow volcano plumbing  
279 reflected in the opening of new effusive vents at progressively lower elevations. The transition between explosive and effusive  
280 regimes was also marked by a clear decrease in the occurrence of VLP events (Fig. 4), and a migration of their source deeper  
281 within the conduit (as reported by the automatic seismic monitoring of INGV Osservatorio Vesuviano:  
282 <http://eolo.ov.ingv.it/eolo/>) and as already observed during past unrest by Ripepe et al. (2015). This contrasts with the flank  
283 eruptions of 2007 and 2014 (Ripepe et al., 2009; 2015) when VLP rates remained high during effusion; in July, 2024 it appears  
284 that effusion reduced the overall explosivity through progressive degassing of the shallow magma rather than recalling fresh,  
285 gas-rich, magma from depth. The new effusive regime, indeed, was characterized by a substantial lack of Strombolian  
286 explosive activity at the surface between 4-11 July, as observed in the field by our research team. The quasi-continuous collapse  
287 activity, observed from 13:00 UTC on 4 July, appeared to be linked to instabilities in the crater area around newly created  
288 vents; this instability persisted in the following days, with the number of events peaking on 5 July (83 recorded occurrences  
289 recorded in a single day (INGV-OE, 2024)). The collapse activity recorded along the N crater rim, adjacent to the SdF, resulted  
290 in significant changes to the morphology of this sector of the volcanic edifice (Fig. 7).

291

#### 292 **4.2 Eruptive activity during the second week of July, 2024.**

293 The effusive regime, that began on 4 July, ended with the occurrence of the paroxysmal explosion on 11 July. The explosion  
294 generated an infrasonic pressure of 115 Pa at station STR6 with an associated VLP peak amplitude of  $5.8 \times 10^{-5} \text{ ms}^{-1}$  (see Fig.  
295 3S). The associated ash plume reached a height of 5 km above the vent, and pyroclastic flows moved down the SdF. After that,  
296 volcanic activity reduced its intensity, accompanied by low levels of tremor and VLP events; tremor increased again on 12  
297 July, associated with emplacement of a small lava flow.

298 The eruptive crisis of July 2024, culminating into the 11 July paroxysm, is consistent with previous eruptions at Stromboli,  
299 such as those in April 2003, March 2007, and July-August 2019. The observations that we have presented in this manuscript  
300 can be used to inform a conceptual model of the entire sequence of processes responsible for the observed surface and eruptive  
301 activity, within the framework of previous studies (e.g., James et al., 2006; Chouet et al., 2008; Del Bello et al., 2012; Suckale  
302 et al., 2015; McKee et al., 2022).

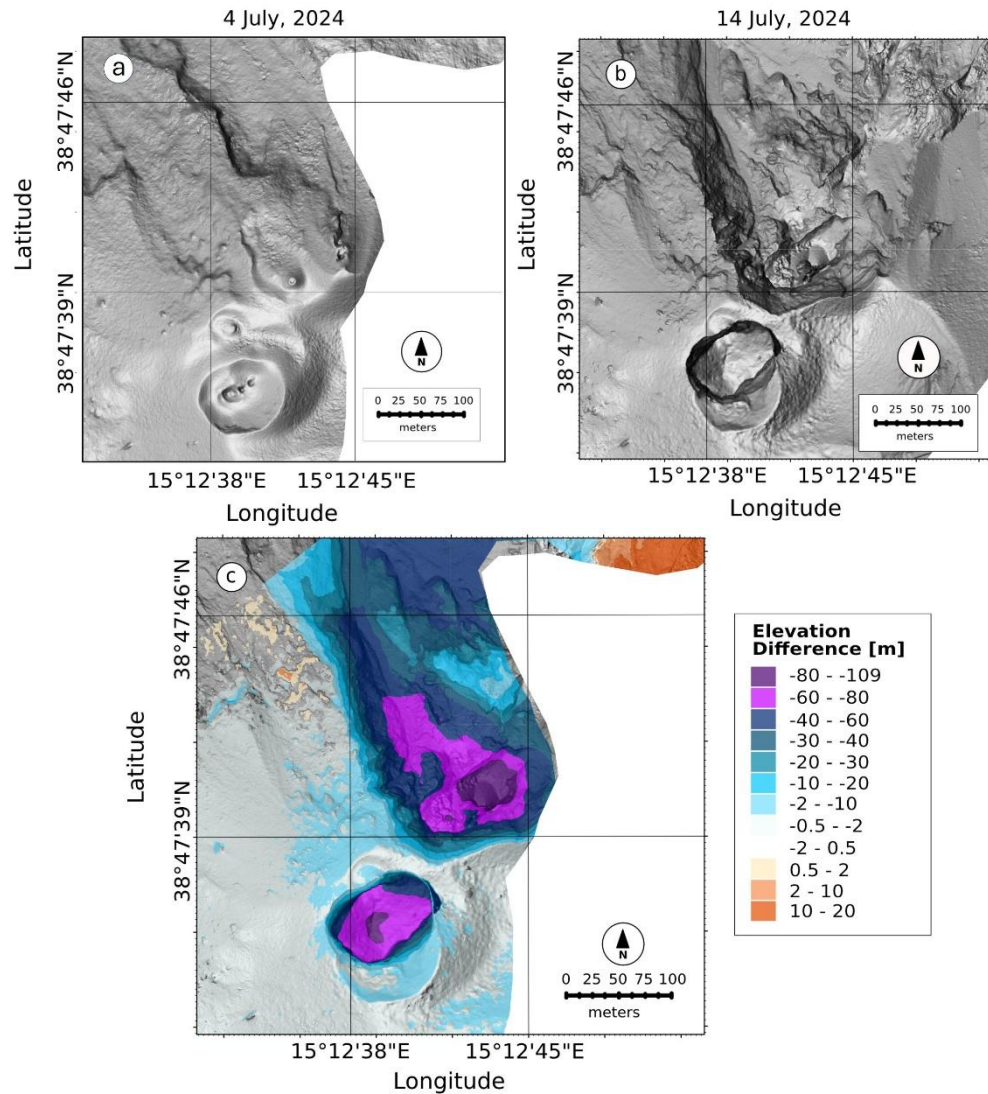
303 At the more explosive end of the spectrum of Strombolian activity major explosions and paroxysms are often explained  
304 invoking the "slug model" (James et al., 2006; Chouet et al., 2008; Del Bello et al., 2012). In this model, gas bubbles (slugs)  
305 form deeper in the magma column and gradually coalesce as they rise through the conduit due to an increase of the magma  
306 viscosity. As gas slugs ascend, they expand due to the decreasing confining pressure and eventually reach the surface. When  
307 they burst at the top of the magma column, they release gas explosively, fragmenting the magma and producing pyroclasts and  
308 feeding ash plumes of varying sizes. After the major explosion on 4 July, an effusive regime was established, characterized by

309 lava flows, during which more degassed magma was erupted. Following the initial explosive activity driven by gas slugs, we  
 310 infer that the transition to **the** effusive regime **was** controlled by depressurization of the shallow plumbing system similar to  
 311 **the model of** Ripepe et al. (2017). The depressurization of the system caused by the initial explosive activity allowed magma  
 312 to flow and reach the surface forming lava flows, without further explosive activity. As the shallow volcanic conduit  
 313 progressively emptied it **led** to structural instability, causing collapses and landslides along the SdF.  
 314 According to Ripepe et al. (2017), the emptying of the conduit creates a “vacuum” effect that draws more gas-rich magma  
 315 from deeper within the system. As volatile-rich magma rises and **experiences** lower pressures, **activity can be triggered,**  
 316 **sometimes** resulting in a paroxysmal event. The dynamics of the 11<sup>th</sup> July paroxysmal explosion **shared similarities** across  
 317 seismic, acoustic, and deformation parameters **with past events** (Genco and Ripepe, 2010; Ripepe et al., 2021a). This  
 318 consistency further validates the established models **of activity and Stromboli**, where the largest explosions and energetic  
 319 events, such as paroxysms, are driven by the same source mechanism. The scale-invariant conduit dynamics of ground  
 320 deformation demonstrate that inflation amplitude and duration scale directly with the magnitude of the explosion (Ripepe et  
 321 al., 2021a). Ground deformation observed on 11<sup>th</sup> July (Fig. 6) follows the same exponential inflation pattern as seen in previous  
 322 paroxysms (Ripepe et al., 2021a). This **behaviour** is typically explained by bubble dynamics, where the pressure on the conduit  
 323 walls increases due to the rapid volumetric expansion of gas in highly vesiculated magma. As gas rises and expands, it pushes  
 324 the magma column toward the surface, often leading to precursory lava emissions from the vent. Ground deformation is likely  
 325 caused by a combination of increasing magma static pressure and the pressurization of degassed magma at the top of the  
 326 column, driven by the exponential **expansion of the gas phase**. When the pressure applied by the gas-rich magma exceeds the  
 327 tensile strength of the viscous magma plug, fragmentation occurs, resulting in the explosive release of gas and pyroclastic  
 328 material (e.g. paroxysm). Another possible mechanism, proposed by Suckale et al. (2016) and McKee et al., (2022) suggests  
 329 that the explosion is triggered by the rapid expansion and release of gas when a partial rupture occurs in the plug at the top of  
 330 the magma column.

### 331 332 **4.3 Morphological changes of the crater area caused by the explosive activity.**

333 During the study period, we also collected UAS data and compiled very high-resolution repeat DEMs (0.2-0.5 m/pixel), which  
 334 allowed quantifying topographical changes via DEM differencing. The difference between DEMs on 4 July (morning; Civico  
 335 et al., 2025) and **14** July (Civico et al., 2024a,b) is shown in Fig. 7c. The data processing methodology follows procedures  
 336 described in Civico et al. (2022, 2024a). The most notable morphological variations were observed in the afternoon of 4 July,  
 337 while the paroxysm on 11 July did not lead to significant changes.

338 The summit craters **experienced** loss of material due to the opening of two eruptive vents at approximately 700 and 500 m  
 339 a.s.l.. While the CS crater sector showed a roughly circular crater floor deepening of about 84 m, the N sector was affected by  
 340 the complete dismantling of its northern rim and external slope, marking the deepest morphological change **observed** at the  
 341 summit craters in the last decade, with a maximum difference in altitude of 109 m. The total volume loss recorded in the  
 342 summit craters sector was estimated at 3.3 **Mm<sup>3</sup>** (Civico et al., 2024a).



343

344 **Figure 7:** Multidirectional hillshade plots of Stromboli's crater area: a) 4 July, 2024 (Civico et al., 2025), b) 14 July, 2024 (Civico et  
 345 al., 2024a,b), c) map of elevation difference (Dem of Differences) highlighting morphological changes between 4 and 14 July, 2024.  
 346 Purple areas indicate material loss, whereas orange areas indicate material gain.

347 Unlike the summit craters, the subaerial portion of the SdF slope was affected by both accumulation and erosion processes.  
 348 Here, the main loss of material (2.74  $\text{Mm}^3$ ; Civico et al., 2024a) was localized along the canyon formed in October 2022 (Di  
 349 Traglia et al., 2024), which widened and deepened during the July 2024 eruption. On the other hand, accumulation processes  
 350 instead were mainly due to PDC and lava flow deposits within the northeastern sector of the edifice. The maximum  
 351 accumulation of lava occurred at the new lava delta (maximum difference in altitude of 45 m), located in the center of the SdF  
 352 shoreline (Civico et al., 2024a).

354 **5 Conclusion**

355 The eruptive activity at Stromboli starting from 4<sup>th</sup> July, and culminating with a paroxysm on 11 July, 2024, provides a  
356 comprehensive case study of explosive volcanism at open-conduit volcanoes and offers valuable insights into its causative  
357 processes and mechanism.

358 The July 2024 paroxysm was preceded by a prolonged phase of heightened activity, characterized by increased volcanic tremor  
359 and VLP events. The elevated levels of seismicity, combined with observed crater rim collapses and lava flows, suggest a  
360 progressive destabilization of the volcanic edifice. In particular, the major explosion on 4 July, and the subsequent paroxysm  
361 on 11 July highlight the role of magma gas dynamics, where increased gas volumes and pressure led to significant eruptive  
362 events.

363 Analysis of the seismic records reveals that the volcanic tremor intensity is linked to gas-rich magma movement, reaching in  
364 this eruptive sequence unprecedented values at Stromboli. However, the variability in VLP events indicates that, while useful  
365 for monitoring overall volcanic unrest, these signals alone may not serve as reliable precursors for major explosive events.  
366 Instead, the combined analysis of different geophysical parameters, including ground deformation, proved crucial for early  
367 warning and forecasting as previously suggested by Ripepe et al. (2021a).

368 Ground deformation patterns, specifically the inflation-deflation cycle observed before explosions, align with previous studies,  
369 confirming that such patterns reflect the occurrence of imminent explosions regardless of their magnitude. The exponential  
370 inflation observed before the paroxysm, caused by gas expansion and the rise of slugs within the magma column, is the same  
371 as in other paroxysmal events at Stromboli.

372 Through UAS data, Civico et al. (2024a) were able to estimate a total volume loss of about 6.0 Mm<sup>3</sup> involved after the  
373 gravitational mass collapses occurred on 4 and 11 July. The partial collapses generated a reshaping of the summit craters area  
374 as well as a deepening 2022 canyon along SdF, thus increasing flank instability.

375 In conclusion, our results demonstrate how geophysical, visual observation and UAS-derived topographic data offer new,  
376 valuable, insights for tracking and characterizing the processes that control the onset of volcanic explosive activity at Stromboli  
377 and other similar volcanoes. We suggest that multi-parameter volcano monitoring will lead to further significant advances in  
378 volcanic hazard mitigation.

379 **Data availability**

380 Seismic waveform data used in this study are from the INGV seismic network. All data are publicly available from EIDA Italia  
381 (<https://eida.ingv.it/>). Infrasound data are available upon request from the INGV- Osservatorio Vesuviano or direct enquiry to



382 the authors of this manuscript. The infrasound data from PISA station are available at  
383 <https://doi.org/10.5281/zenodo.14245572>.

384 **Author contribution**

385 L.Z., S.D.A. and P.S. wrote the research proposals that funded the installation and maintenance of the infrasound array and  
386 UAS, designed the field experiment, and financially supported this publication. L.Z. and S.D.A. tested the infrasonic  
387 equipment, organized fieldwork and participated in the original design of the experiment. L.Z., S.D.A., R.C., T.R. contributed  
388 to assembling the final multiparametric dataset and tested its quality and retrieval. L.Z., R.C. and T.R. installed and maintained  
389 the equipment during the field acquisition. L.Z, S.D.A. and D.G. performed analyses of infrasound data, seismic and tilt data,  
390 and prepared all figures. R.C. and T.R. acquired and analysed the UAS images. L.Z. D.G. and S.D.A. jointly wrote the initial  
391 draft of the manuscript and all authors contributed to review and edit the final version.

392 **Competing interests**

393 The authors declare that they have no conflict of interest.

394 **Acknowledgements**

395 INGV Project ‘Pianeta Dinamico (Dynamic Planet) - Working Earth’: Geosciences For The Understanding The Dynamics Of  
396 The Earth And The Consequent Natural Risks - “Dynamo - DYNAmics of eruptive phenoMena at basaltic vOlcanoes”  
397 (<https://progetti.ingv.it/it/pian-din/dynamo#project-info>).

398 INGV Departmental Strategic Project “UNO - UNderstanding the Ordinary to forecast the extraordinary: An integrated  
399 approach for studying and interpreting the explosive activity at Stromboli volcano” (<https://progetti.ingv.it/it/uno-stromboli>).

400 L.Z., D.G., S.D.A., R.C., T. R: and P.G. are supported by the grant "Progetto INGV Pianeta Dinamico" - Sub-project  
401 VT\_DYNAMO 2023 - code CUP D53J19000170001 - funded by Italian Ministry MIUR (“Fondo Finalizzato al rilancio degli  
402 investimenti delle amministrazioni centrali dello Stato e allo sviluppo del Paese”, legge 145/2018).

403 We are indebted to all the INGV colleagues who have contributed to the monitoring efforts on Stromboli during July 2024 and  
404 the ones involved in the surveillance and network maintenance activities, to Maria Zagari (Italian Civil Aviation Authority -  
405 ENAC) for her help in issuing new NOTAMs during the emergency, and to Giuseppe De Rosa, Istituto Nazionale di  
406 Oceanografia e di Geofisica Sperimentale (OGS) for providing the photo of the 11 July paroxysm in Fig. 1.

407 The contents of this article represent the authors’ ideas and do not necessarily correspond to the official opinion and policies  
408 of the Dipartimento della Protezione Civile - Presidenza del Consiglio dei Ministri. We are grateful to the colleagues of INGV  
409 -Osservatorio Vesuviano- for their support in the data management.



## 410 **Financial support**

411 This work was supported by the grant "Progetto INGV Pianeta Dinamico" - Sub-project VT\_DYNAMO 2023- code CUP  
412 D53J19000170001 - funded by Italian Ministry MIUR ("Fondo Finalizzato al rilancio degli investimenti delle amministrazioni  
413 centrali dello Stato e allo sviluppo del Paese", legge 145/2018) and by INGV Departmental Strategic Project "UNO -  
414 UNDERstanding the Ordinary to forecast the extraordinary: An integrated approach for studying and interpreting the explosive  
415 activity at Stromboli volcano".

## 416 **References**

417 Aiuppa, A., Burton, M., Caltabiano, T., Giudice, G., Guerrieri, S., Liuzzo, M., and Salerno, G.: Unusually large magmatic  
418 CO<sub>2</sub> gas emissions prior to a basaltic paroxysm, *Geophys. Res. Lett.*, 37, <https://doi.org/10.1029/2010GL044997>, 2010.  
419 Andronico, D., Del Bello, E., D’Orlando, C., Landi, P., Pardini, F., Scarlato, P., and Valentini, F.: Uncovering the eruptive  
420 patterns of the 2019 double paroxysm eruption crisis of Stromboli volcano, *Nat. Commun.*, 12, [https://doi.org/10.1038/s41467-](https://doi.org/10.1038/s41467-021-23349-4)  
421 021-23349-4, 2021.  
422 Bertagnini, A., Métrich, N., Landi, P., and Rosi, M.: Stromboli volcano (Aeolian Archipelago, Italy): An open window on the  
423 deep-feeding system of a steady state basaltic volcano, *J. Geophys. Res. Solid Earth*, 108,  
424 <https://doi.org/10.1029/2002JB002146>, 2003.  
425 Bonaccorso, A.: Evidence of a dyke-sheet intrusion at Stromboli Volcano inferred through continuous tilt, *Geophys. Res. Lett.*,  
426 25, <https://doi.org/10.1029/98GL00766>, 1998.  
427 Burton, M., Allard, P., Murè, F., and La Spina, A.: Magmatic gas composition reveals the source depth of slug-driven  
428 Strombolian explosive activity, *Science*, 317, <https://doi.org/10.1126/science.1141900>, 2007.  
429 Calvari, S., Spampinato, L., and Lodato, L.: The 5 April 2003 vulcanian paroxysmal explosion at Stromboli volcano (Italy)  
430 from field observations and thermal data, *J. Volcanol. Geotherm. Res.*, 149, <https://doi.org/10.1016/j.jvolgeores.2005.09.008>,  
431 2006.  
432 Calvari, S., Spampinato, L., Bonaccorso, A., Oppenheimer, C., Rivalta, E., and Boschi, E.: Lava effusion—A slow fuse for  
433 paroxysms at Stromboli volcano? *Earth Planet. Sci. Lett.*, <https://doi.org/10.1016/j.epsl.2011.03.005>, 2011.  
434 Calvari, S., and Nunnari, G.: Statistical insights on the eruptive activity at Stromboli volcano (Italy) recorded from 1879 to  
435 2023, *Remote Sensing*, 15, <https://doi.org/10.3390/rs15174298>, 2023.  
436 Caricchi, L., Montagna, C. P., Aiuppa, A., Lages, J., Tamburello, G., and Papale, P.: CO<sub>2</sub> flushing triggers paroxysmal  
437 eruptions at open conduit basaltic volcanoes, *J. Geophys. Res.: Solid Earth*, 129, <https://doi.org/10.1029/2023JB02561>, 2024.  
438 Chouet, B., Saccorotti, G., Martini, M., Dawson, P., De Luca, G., Milana, G., and Scarpa, R.: Source and path effects in the  
439 wave fields of tremor and explosions at Stromboli Volcano, Italy, *J. Geophys. Res.: Solid Earth*, 102,  
440 <https://doi.org/10.1029/96JB03395>, 1997.

441 Chouet, B., Dawson, P., Ohminato, T., Martini, M., Saccorotti, G., Giudicepietro, F., De Luca, G., Milana, G., and Scarpa, R.:  
 442 Source mechanisms of explosions at Stromboli Volcano, Italy, determined from moment-tensor inversions of very-long-period  
 443 data, *J. Geophys. Res.: Solid Earth*, 108, <https://doi.org/10.1029/2002JB001919>, 2003.  
 444 Chouet, B., Dawson, P., and Martini, M.: Shallow-conduit dynamics at Stromboli Volcano, Italy, imaged from waveform  
 445 inversions, *Geol. Soc. London, Special Publications*, 307, <https://doi.org/10.1144/SP307.5>, 2008.  
 446 Colò, L., Ripepe, M., Baker, D. R., and Polacci, M.: Magma vesiculation and infrasonic activity at Stromboli open conduit  
 447 volcano, *Earth Planet. Sci. Lett.*, 292, <https://doi.org/10.1016/j.epsl.2010.01.041>, 2010.  
 448 Civico, R., Ricci, T., Scarlato, P., Andronico, D., Cantarero, M., Carr, B. B., De Beni, E., Del Bello, E., Johnson, J. B.,  
 449 Kueppers, U., Pizzimenti, L., Schmid, M., Strehlow, K., and Taddeucci, J.: Unoccupied Aircraft Systems (UASs) Reveal the  
 450 Morphological Changes at Stromboli Volcano (Italy) before, between, and after the 3 July and 28 August 2019 Paroxysmal  
 451 Eruptions, *Remote Sensing*, 13, <https://doi.org/10.3390/rs13010141>, 2021.  
 452 Civico, R., Ricci, T., Cecili, A., and Scarlato, P.: High-resolution topography reveals morphological changes of Stromboli  
 453 volcano following the July 2024 eruption, *Sci. Data*, 11, 1219, <https://doi.org/10.1038/s41597-024-04098-y>, 2024a.  
 454 Civico, R., Ricci, T., Scarlato, P.: High-Resolution SfM Topography of Stromboli volcano (Italy), 14 July 2024.  
 455 OpenTopography. <https://doi.org/10.5069/G9S75DJH>, 2024b. Accessed: 2025-02-05  
 456 Civico, R., Ricci, T., Scarlato, P.: SfM Topography of Stromboli volcano (Italy), 04 July 2024 – crater terrace.  
 457 OpenTopography. <https://doi.org/10.5069/G9T151WP>, 2025. Accessed: 2025-02-05  
 458 D’Auria, L., Giudicepietro, F., Martini, M., and Peluso, R.: Seismological insight into the kinematics of the 5 April 2003  
 459 vulcanian explosion at Stromboli volcano (southern Italy), *Geophys. Res. Lett.*, 33, <https://doi.org/10.1029/2005GL025502>,  
 460 2006.  
 461 De Angelis, S., and Bodin, P.: Watching the Wind: Seismic Data Contamination at Long Periods due to Atmospheric Pressure-  
 462 Field-Induced Tilting, *Bull. Seismol. Soc. Am.*, 102, <https://doi.org/10.1785/0120110245>, 2012.  
 463 Del Bello, E., Llewellyn, E. W., Taddeucci, J., Scarlato, P., and Lane, S. J.: An analytical model for gas overpressure in slug-  
 464 driven explosions: Insights into Strombolian volcanic eruptions, *J. Geophys. Res.: Solid Earth*, 117(B2),  
 465 <https://doi.org/10.1029/2011JB008747>, 2012.  
 466 Diaz-Moreno, A., Iezzi, A. M., Lamb, O. D., Fee, D., Kim, K., Zuccarello, L., and De Angelis, S.: Volume Flow Rate  
 467 Estimation for Small Explosions at Mt. Etna, Italy, From Acoustic Waveform Inversion, *Geophys. Res. Lett.*, 46,  
 468 <https://doi.org/10.1029/2019GL084159>, 2019.  
 469 Di Traglia, F., Berardino, P., Borselli, L., Calabria, P., Calvari, S., Casalbore, D., et al.: Generation of deposit-derived  
 470 pyroclastic density currents by repeated crater rim failures at Stromboli Volcano (Italy), *Bull. Volcanol.*, 86,  
 471 <https://doi.org/10.1007/s00445-024-01516-0>, 2024.  
 472 Delle Donne, D., Tamburello, G., Aiuppa, A., Bitetto, M., Lacanna, G., D’Aleo, R., and Ripepe, M.: Exploring the explosive-  
 473 effusive transition using permanent ultraviolet cameras, *J. Geophys. Res.: Solid Earth*, 122(6), 4377–4394,  
 474 <https://doi.org/10.1002/2017JB014027>, 2017.

European Centre for Medium-Range Weather Forecasts (ECMWF), ECMWF Reanalysis v5. Available at: <https://www.ecmwf.int/en/forecasts/dataset/ecmwf-reanalysis-v5>. Access date: 21 July 2024.

Fee, D., Izbekov, P., Kim, K., Yokoo, A., Lopez, T., Prata, F., Kazahaya, R., Nakamichi, H., and Iguchi, M.: Eruption mass estimation using infrasound waveform inversion and ash and gas measurements: Evaluation at Sakurajima Volcano, Japan, *Earth Planet. Sci. Lett.*, 480, <https://doi.org/10.1016/j.epsl.2017.09.043>, 2017.

Fee, D., Toney, L., Kim, K., Sanderson, R. W., Iezzi, A. M., Matoza, R. S., De Angelis, S., Jolly, A. D., Lyons, J. J., and Haney, M. M.: Local Explosion Detection and Infrasound Localization by Reverse Time Migration Using 3-D Finite-Difference Wave Propagation, *Front. Earth Sci.*, 9, <https://doi.org/10.3389/feart.2021.640202>, 2021.

Francalanci, L., Tommasini, S., and Conticelli, S.: The volcanic activity of Stromboli in the 1906–1998 AD period: mineralogical, geochemical and isotope data relevant to the understanding of the plumbing system, *J. Volcanol. Geotherm. Res.*, 131, [https://doi.org/10.1016/S0377-0273\(03\)00364-1](https://doi.org/10.1016/S0377-0273(03)00364-1), 2004.

Francalanci, L., Davies, G. R., Lustenhouwer, W., Tommasini, S., Mason, P. R. D., and Conticelli, S.: Intra-Grain Sr Isotope Evidence for Crystal Recycling and Multiple Magma Reservoirs in the Recent Activity of Stromboli Volcano, Southern Italy, *J. Petrol.*, 46, <https://doi.org/10.1093/petrology/egi062>, 2005.

Genco, R., and Ripepe, M.: Inflation-deflation cycles revealed by tilt and seismic records at Stromboli volcano, *Geophys. Res. Lett.*, 37, <https://doi.org/10.1029/2009GL042925>, 2010.

Giordano, G., and De Astis, G.: The summer 2019 basaltic Vulcanian eruptions (paroxysms) of Stromboli, *Bull. Volcanol.*, 83, <https://doi.org/10.1007/s00445-020-01403-0>, 2020.

Giudicepietro, F., Calvari, S., De Cesare, W., Di Lieto, B., Di Traglia, F., Esposito, A. M., Orazi, M., Romano, P., Tramelli, A., Nolesini, T., Casagli, N., Calabria, P., and Macedonio, G.: Seismic and thermal precursors of crater collapses and overflows at Stromboli volcano, *Sci. Rep.*, 13, <https://doi.org/doi.org/10.1038/s41598-023-38205-7>, 2023.

Giudicepietro, F., López, C., Macedonio, G., Alparone, S., Bianco, F., Calvari, S., ... and Tramelli, A.: Geophysical precursors of the July-August 2019 paroxysmal eruptive phase and their implications for Stromboli volcano (Italy) monitoring, *Sci. Rep.*, 10, 10296, <https://doi.org/10.1038/s41598-020-67220-1>, 2020.

Gheri, D., Zuccarello, L., De Angelis, S., Ricci, T., and Civico, R.: Infrasonic Data from the July 4–11, 2024 Paroxysm of Stromboli Volcano [Data set]. Zenodo. <https://doi.org/10.5281/zenodo.14245572>, 2024.

Gurioli, L., Harris, A. J. L., Colò, L., Bernard, J., Favalli, M., Ripepe, M., and Andronico, D.: Classification, landing distribution, and associated flight parameters for a bomb field emplaced during a single major explosion at Stromboli, Italy, *Geology*, 41, <https://doi.org/10.1130/G33576.1>, 2013.

Harris, A., and Ripepe, M.: Temperature and dynamics of degassing at Stromboli, *J. Geophys. Res.: Solid Earth*, 112(B3), <https://doi.org/10.1029/2006JB004393>, 2007.

INGV Bulletin of 25/06/2024: <https://www.ct.ingv.it/index.php/monitoraggio-e-sorveglianza/prodotti-del-monitoraggio/bollettini-settimanali-multidisciplinari/914-bollettino-Settimanale-sul-monitoraggio-vulcanico-geochimico-e-sismico-del-vulcano-Stromboli-del-2024-06-25/file>, last access: 19 August 2024.

509 INGV Bulletin of 02/07/2024: [https://www.ct.ingv.it/index.php/monitoraggio-e-sorveglianza/prodotti-del-](https://www.ct.ingv.it/index.php/monitoraggio-e-sorveglianza/prodotti-del-monitoraggio/bollettini-settimanali-multidisciplinari/915-bollettino-Settimanale-sul-monitoraggio-vulcanico-geochimico-e-sismico-del-vulcano-Stromboli-del-2024-07-02/file)  
 510 [monitoraggio/bollettini-settimanali-multidisciplinari/915-bollettino-Settimanale-sul-monitoraggio-vulcanico-geochimico-e-](https://www.ct.ingv.it/index.php/monitoraggio-e-sorveglianza/prodotti-del-monitoraggio/bollettini-settimanali-multidisciplinari/915-bollettino-Settimanale-sul-monitoraggio-vulcanico-geochimico-e-sismico-del-vulcano-Stromboli-del-2024-07-02/file)  
 511 [sismico-del-vulcano-Stromboli-del-2024-07-02/file](https://www.ct.ingv.it/index.php/monitoraggio-e-sorveglianza/prodotti-del-monitoraggio/bollettini-settimanali-multidisciplinari/915-bollettino-Settimanale-sul-monitoraggio-vulcanico-geochimico-e-sismico-del-vulcano-Stromboli-del-2024-07-02/file), last access: 19 August 2024.  
 512 INGV Bulletin of 09/07/2024: [https://www.ct.ingv.it/index.php/monitoraggio-e-sorveglianza/prodotti-del-](https://www.ct.ingv.it/index.php/monitoraggio-e-sorveglianza/prodotti-del-monitoraggio/bollettini-settimanali-multidisciplinari/918-bollettino-Settimanale-sul-monitoraggio-vulcanico-geochimico-e-sismico-del-vulcano-Stromboli-del-2024-07-09/file)  
 513 [monitoraggio/bollettini-settimanali-multidisciplinari/918-bollettino-Settimanale-sul-monitoraggio-vulcanico-geochimico-e-](https://www.ct.ingv.it/index.php/monitoraggio-e-sorveglianza/prodotti-del-monitoraggio/bollettini-settimanali-multidisciplinari/918-bollettino-Settimanale-sul-monitoraggio-vulcanico-geochimico-e-sismico-del-vulcano-Stromboli-del-2024-07-09/file)  
 514 [sismico-del-vulcano-Stromboli-del-2024-07-09/file](https://www.ct.ingv.it/index.php/monitoraggio-e-sorveglianza/prodotti-del-monitoraggio/bollettini-settimanali-multidisciplinari/918-bollettino-Settimanale-sul-monitoraggio-vulcanico-geochimico-e-sismico-del-vulcano-Stromboli-del-2024-07-09/file), last access: 19 August 2024.  
 515 INGV Bulletin of 16/07/2024: [https://www.ct.ingv.it/index.php/monitoraggio-e-sorveglianza/prodotti-del-](https://www.ct.ingv.it/index.php/monitoraggio-e-sorveglianza/prodotti-del-monitoraggio/bollettini-settimanali-multidisciplinari/920-bollettino-Settimanale-sul-monitoraggio-vulcanico-geochimico-e-sismico-del-vulcano-Stromboli-del-2024-07-16/file)  
 516 [monitoraggio/bollettini-settimanali-multidisciplinari/920-bollettino-Settimanale-sul-monitoraggio-vulcanico-geochimico-e-](https://www.ct.ingv.it/index.php/monitoraggio-e-sorveglianza/prodotti-del-monitoraggio/bollettini-settimanali-multidisciplinari/920-bollettino-Settimanale-sul-monitoraggio-vulcanico-geochimico-e-sismico-del-vulcano-Stromboli-del-2024-07-16/file)  
 517 [sismico-del-vulcano-Stromboli-del-2024-07-16/file](https://www.ct.ingv.it/index.php/monitoraggio-e-sorveglianza/prodotti-del-monitoraggio/bollettini-settimanali-multidisciplinari/920-bollettino-Settimanale-sul-monitoraggio-vulcanico-geochimico-e-sismico-del-vulcano-Stromboli-del-2024-07-16/file), last access: 19 August 2024.  
 518 James, M. R., Lane, S. J., and Chouet, B. A.: Gas slug ascent through changes in conduit diameter: Laboratory insights into a  
 519 volcano-seismic source process in low-viscosity magmas, *J. Geophys. Res.: Solid Earth*, 111,  
 520 <https://doi.org/10.1029/2005JB003718>, 2006.  
 521 Kim, K., and Lees, J. M.: Local Volcano Infrasound and Source Localization Investigated by 3D Simulation, *Seismol. Res.*  
 522 *Lett.*, 85, <https://doi.org/10.1785/0220130135>, 2014.  
 523 Legrand, D., and Pertou, M.: What are VLP signals at Stromboli volcano? *J. Volcanol. Geotherm. Res.*, 421,  
 524 <https://doi.org/10.1016/j.jvolgeores.2021.107429>, 2022.  
 525 Longo, R., Lacanna, G., Innocenti, L., and Ripepe, M.: Artificial Intelligence and Machine Learning Tools for Improving Early  
 526 Warning Systems of Volcanic Eruptions: The Case of Stromboli, *IEEE Trans. Pattern Anal. Mach. Intell.*, 46(12), 7973–7982,  
 527 <https://doi.org/10.1109/TPAMI.2024.3399689>, 2024.  
 528 Marchetti, E., and Ripepe, M.: Stability of the seismic source during effusive and explosive activity at Stromboli Volcano,  
 529 *Geophys. Res. Lett.*, 32, <https://doi.org/10.1029/2005GL023962>, 2005.  
 530 Marchetti, E., Genco, R., and Ripepe, M.: Ground deformation and seismicity related to the propagation and drainage of the  
 531 dyke feeding system during the 2007 effusive eruption at Stromboli volcano (Italy), *J. Volcanol. Geotherm. Res.*, 182,  
 532 <https://doi.org/10.1016/j.jvolgeores.2009.01.029>, 2009.  
 533 McKee, K. F., Roman, D. C., Waite, G. P., and Fee, D.: Silent very long period seismic events (VLPs) at Stromboli Volcano,  
 534 Italy, *Geophys. Res. Lett.*, 49(23), e2022GL100735, <https://doi.org/10.1029/2022GL100735>, 2022.  
 535 McNutt, S. R., and Nishimura, T.: Volcanic tremor during eruptions: Temporal characteristics, scaling and constraints on  
 536 conduit size and processes, *J. Volcanol. Geotherm. Res.*, 178, <https://doi.org/10.1016/j.jvolgeores.2008.07.023>, 2008.  
 537 Pino, N. A., Moretti, R., Allard, P., and Boschi, E.: Seismic precursors of a basaltic paroxysmal explosion track deep gas  
 538 accumulation and slug upraise, *J. Geophys. Res.: Solid Earth*, 116, <https://doi.org/10.1029/2011JB008547>, 2011.  
 539 Pistolesi, M., Delle Donne, D., Pioli, L., Rosi, M., and Ripepe, M.: The 15 March 2007 explosive crisis at Stromboli volcano,  
 540 Italy: Assessing physical parameters through a multidisciplinary approach, *J. Geophys. Res.*, 116,  
 541 <https://doi.org/10.1029/2011JB008527>, 2011.

542 Ripepe, M.: Evidence for gas influence on volcanic seismic signals recorded at Stromboli, *J. Volcanol. Geotherm. Res.*, 70,  
543 [https://doi.org/10.1016/0377-0273\(96\)00033-8](https://doi.org/10.1016/0377-0273(96)00033-8), 1996a.

544 Ripepe, M., Poggi, P., Braun, T., and Gordeev, E.: Infrasonic waves and volcanic tremor at Stromboli, *Geophys. Res. Lett.*,  
545 23, <https://doi.org/10.1029/96GL02394>, 1996b.

546 Ripepe, M., and Gordeev, E.: Gas bubble dynamics model for shallow volcanic tremor at Stromboli, *J. Geophys. Res.: Solid*  
547 *Earth*, 104, <https://doi.org/10.1029/1998JB900046>, 1999.

548 Ripepe, M., Delle Donne, D., Lacanna, G., Marchetti, E., and Olivieri, G.: The onset of the 2007 Stromboli effusive eruption  
549 recorded by an integrated geophysical network, *J. Volcanol. Geotherm. Res.*, 182(3-4), 131–136,  
550 <https://doi.org/10.1016/j.jvolgeores.2009.02.011>, 2009.

551 Ripepe, M., Delle Donne, D., Genco, R., Maggio, G., Pistolesi, M., Marchetti, E., Lacanna, G., Olivieri, G., and Poggi, P.:  
552 Volcano seismicity and ground deformation unveil the gravity-driven magma discharge dynamics of a volcanic eruption, *Nat.*  
553 *Commun.*, 6(1), 6998, <https://doi.org/10.1038/ncomms7998>, 2015.

554 Ripepe, M., Pistolesi, M., Coppola, D., Delle Donne, D., Genco, R., Lacanna, G., ... and Valade, S.: Forecasting effusive  
555 dynamics and decompression rates by magmastatic model at open-vent volcanoes, *Sci. Rep.*, 7,  
556 <https://doi.org/10.1038/s41598-017-00748-4>, 2017.

557 Ripepe, M., Lacanna, G., Pistolesi, M., Silengo, M. C., Aiuppa, A., Laiolo, M., ... and Delle Donne, D.: Ground deformation  
558 reveals the scale-invariant conduit dynamics driving explosive basaltic eruptions, *Nat. Commun.*, 12, 1683,  
559 <https://doi.org/10.1038/s41467-021-21722-2>, 2021a.

560 Ripepe, M., Delle Donne, D., Legrand, D., Valade, S., and Lacanna, G.: Magma pressure discharge induces very long period  
561 seismicity, *Sci. Rep.*, 11, <https://doi.org/10.1038/s41598-021-86061-x>, 2021b.

562 Ripepe, M., and Lacanna, G.: Volcano generated tsunamis recorded in the near source, *Nat. Commun.*, 15,  
563 <https://doi.org/10.1038/s41467-024-18567-x>, 2024.

564 Rizzo, A. L., Federico, C., Inguaggiato, S., Sollami, A., Tantiello, M., Vita, F., ... and Grassa, F.: The 2014 effusive eruption at  
565 Stromboli volcano (Italy): Inferences from soil CO<sub>2</sub> flux and <sup>3</sup>He/<sup>4</sup>He ratio in thermal waters, *Geophys. Res. Lett.*, 42,  
566 <https://doi.org/10.1002/2015GL064152>, 2015.

567 Rosi, M., Bertagnini, A., Harris, A. J. L., Pioli, L., Pistolesi, M., and Ripepe, M.: A case history of paroxysmal explosion at  
568 Stromboli: Timing and dynamics of the April 5, 2003 event, *Earth Planet. Sci. Lett.*, 243,  
569 <https://doi.org/10.1016/j.epsl.2006.01.035>, 2006.

570 Rosi, M., Pistolesi, M., Bertagnini, A., Landi, P., Pompilio, M., and Di Roberto, A.: Chapter 14 Stromboli volcano, Aeolian  
571 Islands (Italy): present eruptive activity and hazards, *Geol. Soc., London, Mem.*, 37, <https://doi.org/10.1144/M37.14>, 2013.

572 Sparks, R. S. J.: Dynamics of magma degassing, *Geol. Soc., London, Spec. Publ.*, 213,  
573 <https://doi.org/10.1144/GSL.SP.2003.213.01.07>, 2003.

574 Suckale, J., Keller, T., Cashman, K. V., and Persson, P.-O.: Flow-to-fracture transition in a volcanic mush plug may govern  
575 normal eruptions at Stromboli, *Geophys. Res. Lett.*, 43, <https://doi.org/10.1002/2016GL068082>, 2016.

576 Wang, S.: Finite-difference time-domain approach to underwater acoustic scattering problems, J. Acoust. Soc. Am., 99,  
577 <https://doi.org/10.1121/1.414620>, 1996.